THE APPLICATION OF ALUMINUM FOAM FOR THE HEAT AND NOISE REDUCTION IN AUTOMOBILES

A Thesis Submitted to
the Graduate School of Engineering and Sciences of
İzmir Institute of Technology
in Partial Fulfillment of the Requirements for the Degree of

MASTER OF SCIENCE

in Mechanical Engineering

by
Ilgaz AKSELİ

June 2005
İZMİR

We approve the thesis of **Ilgaz AKSELİ**

                                                                Date of Signature

....   **24 June 2005**
Assoc. Prof. Dr. Mustafa GÜDEN
Supervisor
Department of Mechanical Engineering
İzmir Institute of Technology

....   **24 June 2005**
Prof. Dr. Zafer İLKEN
Co-Supervisor
Department of Mechanical Engineering
İzmir Institute of Technology

....   **24 June 2005**
Assoc. Prof. Dr. Metin TANOĞLU
Department of Mechanical Engineering
İzmir Institute of Technology

....   **24 June 2005**
Asst. Prof. Dr. Aytunç EREK
Department of Mechanical Engineering
Dokuz Eylül University

....   **24 June 2005**
Asst. Prof. Dr. Tahsin BAŞARAN
Department of Mechanical Engineering
Dokuz Eylül University

....
Assoc. Prof. Dr. Semahat ÖZDEMİR
Head of the Graduate School

ACKNOWLEDGEMENTS

ABSTRACT

An experimental study has been conducted to investigate the effective thermal conductivity and sound absorption coefficient of Al and $SiC_{particle}$/Al closed-cell foams. The foams were prepared using the foaming of powder compact processes developed by Fraunhofer CMAM. The foaming of powder compact process has been extended for the foaming of composite compacts containing 10 weight percent of SiC particles. Effective thermal conductivity measurements were performed using the temperature distribution for steady state conduction through a uniform plane wall method. The sound absorption coefficient measurements were conducted using the standing wave ratio method. The effect of hole drilling on the sound absorption coefficient of foams was also investigated. The measured effective thermal conductivities of the foams were also fitted to the previously developed effective thermal conductivity models of metal foams. The effective thermal conductivities of studied Al foams were then expressed as function of percent porosity with the best-fitted model equation. The effective thermal conductivity values of Al foams were also compared with those of Alporas closed and ERG open cell foams produced by the foaming of Al melt and investment casting methods, respectively. The sound absorption coefficients of Al and SiC/Al foams were found relatively low and similar at lower relative densities and frequencies. Hole drilling was found to be effective in increasing sound absorption values of foam above 400 Hz. The sound absorption in Al and SiC/Al foams was further explained based on the viscous losses and thermal damping effects.

ÖZET

Toz tabletlerden köpükleştirme yöntemi ile SiC-parçacık (SiC_p) katkılı kapalı hücreli alüminyum (Al) ve saf alüminyumdan elde edilen köpüklerin efektif ısıl iletkenlikleri ve ses emme katsayılarını belirlemek için deneysel bir çalışma yapılmıştır. Köpükler üzerinde belirli ölçülerde delik delmenin de ses emme katsayısına etkisi incelenmiştir. SiC-parçacıklarının takviyesi ile kapalı hücreli alüminyum köpüğün efektif ısıl iletkenliğinde düşüş görülmüştür. Diğer çalışmalarda bulunmuş teorik formüller kullanılarak efektif ısıl iletkenlik katsayıları hesaplanmış ve sonuçlar karşılaştırılmıştır. Kapalı hücreli Alporas ve açık hücreli ERG köpüklerinin efektif ısıl iletkenlikleri ile karşılaştırma yapılmış ve yapılan karşılaştırmalar sonucu, çalışmada kullanılan kapalı hücreli alüminyum köpüğün daha düşük efektif ısıl iletkenliğe sahip olduğu saptanmıştır.

Göreli yoğunlukları düşük olan SiC-parçacık takviyeli alüminyum ve saf alüminyum köpüklerin düşük frekanslarda benzer ses emme katsayılarına sahip oldukları gözlenmiştir. Ancak yüksek frekanslarda SiC-parçacık takviyeli alüminyum köpüğün ses emme katsayısının yükseldiği görülmüştür. 400 Hz üstündeki frekanslarda delik delme işleminin etkin olduğu, numunelerin yükselen ses emme katsayıları ile belirlenmiştir. Kısmen ince olan kapalı hücreli köpüklerde delik delme işleminin ses emme katsayısına olumlu yönde yarar sağladığı saptanmıştır.

TABLE OF CONTENTS

LIST OF FIGURES

LIST OF TABLES

NOMENCLATURE

A Area of heat transfer surface (m^2)

$\dfrac{dT}{dx}$ Temperature gradient

Q The amount of heat transfer (W)

k Thermal conductivity of the solid material (W/m·K)

L Length of the solid material in the direction of heat flow (m)

ΔT Temperature difference between the ends of the solid material (K)

q' Steady-state heat flux through the material (W/m^2)

T_{cold} Temperature at the cold side of the solid material (K)

T_{hot} Temperature at the hot side of the solid material (K)

x Independent spatial variable in the direction of the material thickness (m)

σ_{sb} Stefan's constant ($W/m^2 \cdot K^4$)

k* Total thermal conduction in a porous system (W/m·K)

k_s The contribution of thermal conductivity from conduction through the solid in a porous system (W/m·K)

k_c Thermal conductivity due to convective processes in a porous system (W/m·K)

k_r The contribution of thermal conductivity from radiation in a porous system (W/m·K)

V_{foam} Volume of the foam, (mm^3)

ρ Solid material density (kg/m^3)

$\rho*$ Foam density (kg/m^3)

ϕ Porosity of the foam material

m Mass of the foam material (kg)

k_e Effective thermal conductivity of the foam (W/m·K)

k_f Thermal conductivity of fluid phase (W/m·K)

$k_{parallel}$ Thermal conduction in parallel mode (W/m·K)

k_{series} Thermal conduction in series mode (W/m·K)

k_{comp} Thermal conductivity of composite material (W/m·K)

k_{bulk} Thermal conductivity of bulk material (W/m·K)

R Simplification quantity ($W^{-1} \cdot m \cdot K$)

e Dimensionless cubic node length

d	Dimensionless foam ligament radius
ζ	Solid conduction efficiency factor
v	Wave speed (m/s)
λ	Wavelength (m)
f	Frequency (Hz)
T	Period (s)
W_{ref}	Reference power (W)
L_W	Sound power level (dB)
W	Total sound power (W)
Lp	Sound pressure level (dB)
p_{ref}	Standard reference pressure (Pa)
p	Sound pressure (dB)
ν	Speed of sound (m/s)
T	Absolute temperature of air in degrees Kelvin (K)
k	Boltzmann's constant (J/K)
B	Bulk modulus (N/m^2)
Y	Young's modulus (N/m^2)
γ	Specific heat ratio (k)
I	Sound intensity (W/m^2)
SWR	Standing wave ratio
R	Reflection coefficient amplitude
α	Absorption coefficient
Z	Surface impedance (Ohms/square)
Δ^*	Sound drop level (dB)
f	Volume fraction

CHAPTER 1

INTRODUCTION AND MOTIVATION

It is a known fact that globally customer appreciation and demand for less noisy and more comfortable products are increasing every year constantly. In the automotive industry for example noise and heat conduction control are becoming important design criteria mainly driven by competitive nature of the market and increasing customer awareness. In addition, the increasing demands of decreasing exterior noise emissions, engine and tire noise are further required by the European Union (EU). Therefore, nowadays it is inevitable to optimize the interior and exterior noise and exterior heat level of exhaust system and engines of vehicles. It is well known that exterior noise emission of vehicles is a substantial factor contributing to the environmental acceptance of traffic. Therefore, legislators all over the world have created regulations limiting the exterior noise levels. Exterior noise measurements are carried out by using special test vehicles, which make it possible to study the contribution of each sound source such as engine, gearbox and tires. Noise, vibration and harshness (NVH) analysis and thermal barrier measurements for both power-trains and exhaust systems are routinely performed to the vehicles by the most of the automotive companies and their suppliers. There are also research centers conducting R&D for aiming at identifying and classifying many qualities of unwanted sounds of power-trains and decreasing the exhaust and power-train system's heat conduction to the considerable lower levels.

Stainless steels, fiber felt and more recently polyester fibers (shoddy pad) have so far been used for sound silencers and thermal barrier coating structures in automobiles. In spite of their relatively low cost combined with their excellent ductility, the materials used in them are largely restricted to the most of the automobile models. These structures are typically produced in the form of small sections and individually bonded to the vehicle floor pan. Their functions or properties however can not be tuned up to the particular vehicle interior and exterior regions. In recent years, aluminum started to become preferred material for sound silencers and thermal barrier coatings due to its low weight, being three times less than that of steel. It is now possible to design and manufacture aluminum foam parts showing the same stiffness as steel but

with better sound absorption and thermal barrier capabilities and with significant weight savings as well as simplifying vehicle assembly.

Aluminum and aluminum foam parts could be manufactured in a single piece with a wide range of bulk and surface properties that provide excellent physical, thermal and acoustic characteristics, which will be elaborated in Chapter 4, Chapter 5 and Chapter 6. Sound absorption and thermal barrier coating properties of aluminum foams were studied over the 15 years. In the last decade, aluminum foams were investigated as the potential materials to be used in sound silencers and thermal barriers. Most of the applications however are based on the open cell aluminum foams (interconnected cells) or semi-opened aluminum foams, owing to their better sound and thermal emissions as compared with closed cell foams. On the other hand, the processing cost of closed-cell Al foams are lower than that of open cell foam and with the use of foaming from powder compact process, it also possible to manufacture parts in the final form, in any shape and dimensions with a dense Al skin on it. The dense skin allows the applications of finishing process such as grinding, polishing and painting. Recently, Al foams with SiC_p, showing metal matrix composite structure, have been produced using the foaming from powder compact process. To improve the performance of sound silencers and thermal barrier coatings many absorbing materials, generally foamy and fibrous, are developed. However, the performance of SiC_p/Al foams as sound silencers and thermal barrier coatings has not been investigated yet. Therefore, Al foam and SiC_p/Al foams, proposed in this study, can be an alternative for more conventional materials. Therefore, this study is aimed at determining thermal and sound absorption properties of SiC_p/Al foams. These properties were also compared with those of monolithic alloy foams. Present study therefore provides new information on the sound absorption and thermal conductivity of silicon carbide particulate containing Al foams.

CHAPTER 2

MANUFACTURING METHODS OF CLOSED-CELL ALUMINUM FOAMS

There are number of processing methods that are currently used to manufacture Al foams. These include foaming liquid melts, metallic precursors, foaming of powder compacts and ingots containing blowing agents, (Banhart and Baumeister 1998). All these manufacturing routes have their own relative densities and cell structures.

2.1. Foaming Liquid Metals

Metallic melts can be produced by creating gas bubbles in the liquid provided that the melt has been prepared such that the emerging foam is fairly stable during foaming process. This can be done by adding fine ceramic powders or alloying elements to the melt, which form stabilizing particles, or by other means. Currently there are three known ways of foaming metallic melts: gas injecting into the liquid metal, gas-releasing blowing agents addition into the molten metal and dissolved gas precipitation (Banhart 2000a, Körner and Singer 2000).

2.1.1. Foaming Melts by Gas Injection

The first manufacturing method of foaming aluminum and aluminum alloy melts is based on gas injection into molten metal (Figure 2.1) WEB_1 (2005), (Wadley 2002). Alcan N. Hydro Aluminum in Norway and Cymat Corporations in Canada (Banhart and Baumeister 1998, Banhart 2000a) are the manufacturers, which apply this method to produce Al foams. During this process, SiC, aluminum oxide or magnesium oxide particles are used to enhance the viscosity of the liquid metal and adjust its foaming properties because liquid metals can not easily be foamed by bubbling air through them. Drainage of the liquid down the walls of the bubbles occurs too quickly and the bubbles collapse. However, if a small percentage of these particles are added to the melt, the flow of the liquid metal is impeded sufficiently to stabilize the bubbles. In the next

stage, the gas (air, argon or nitrogen) is injected into molten aluminum by using special rotating impellers or air injection shaft or vibrating nozzles, which constitute gas bubbles in the melt and distribute them uniformly and easily through the melt (Gibson and Simone 1997). The base metal is usually an aluminum alloy. The volume fraction of particles varies from 10% to 20%, and the mean size of the particles ranges between 5 μm and 20 μm. This process allows the production of closed-cell foams of 1 m wide to 0.2 m thick slabs with diameters ranging between 5 mm and 20 mm and the foam relative densities between 0.03-0.1 (Prakash et al. 1995).
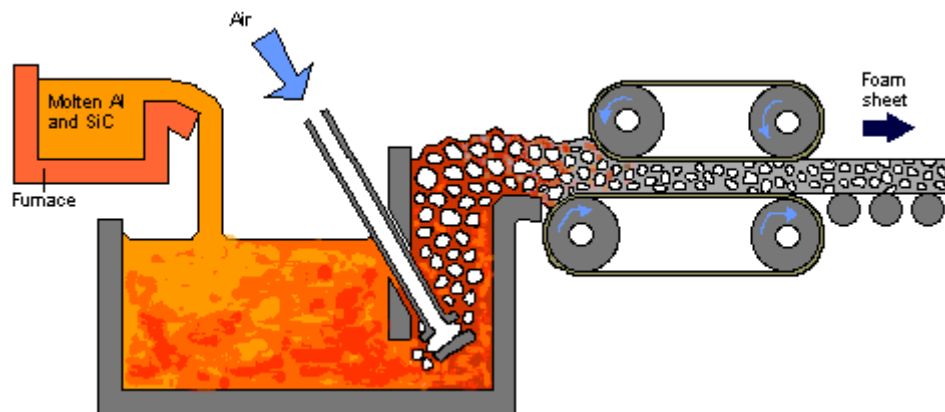
Figure 2.1. Schematic diagram of manufacturing of aluminum foam by melt gas injection method.
(Source: WEB_1, 2005)

The foam is relatively stable owing to the presence of ceramic particles in the melt. The resultant viscous mixture of bubbles and metal melt floats up to the surface of the liquid where it turns into fairly dry liquid foam as the liquid metal drains out. A conveyor belt is used to pull the foam off the liquid surface, and is then left to cool and solidify (Banhart and Baumeister 1998). Many non-metallic reinforcements react with molten metals including alumina, boron carbide, silicon carbide, silicon nitride and boron nitride, but silicon carbide is preferred material in practice (Prakash et al. 1995). Silicon reacts with molten aluminum and forms aluminum carbide and silicon. It has been established that the rate of this reaction can be reduced to an acceptable level by holding the melt at a relatively low temperature during mixing, coating the particles, and inhibiting the reaction by raising the Si content of the aluminum melt. Foaming of melt by gas injection process is the cheapest one among all others, and the only one to

have been as a continuous production. Foam panels can be produced at rates of up to 900 kg/hour. Typical density, average cell size and cell wall thickness are 0.069-0.54 g/cm^3, 3-25 mm, and 50-85 μm, respectively (Gibson and Simone 1997). Average cell size, average cell wall thickness and density can be adjusted by varying processing parameters including gas injection rate and parameters including gas injection rate and rotating shaft speed.
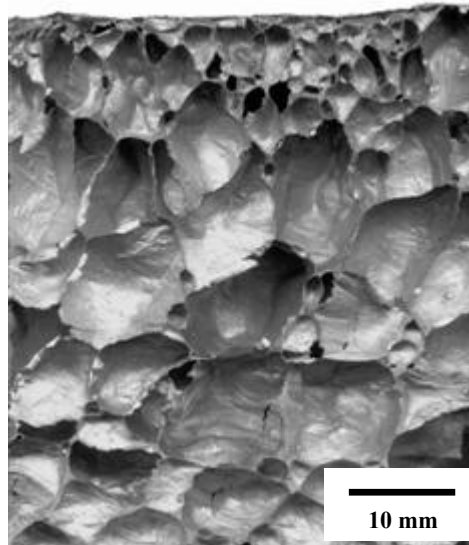
Figure 2.2. Al foam produced by a continuous process of gas injection to a viscous melt, showing the density gradient through the thickness.
(Source: WEB_1, 2005)

The main disadvantage of this process is the poor quality of the foams produced. The cell size is large and often irregular, and the foams tend to have a marked density gradient. Although various methods have been developed to improve the drawing of the foam, the size distribution of the pores is still difficult to control (Figure 2.2) WEB_1 (2005). Besides its low production cost, it may need secondary operations such as machining. The foamed material is either used directly with a closed outer surface, or is cut into the required shape after foaming. Although having high content of ceramic particles, machining of these foams can be problematic. In addition, the pores tend to be tens of millimeters across, while an even and fine structure, like bone structure is more desirable (Banhart 2000b). Advantages of this direct foaming process include the large volume of foam continuously produced and the low densities achieved.

2.1.2. Foaming Melts with Blowing Agents

Adding a blowing agent into the melt is the other way of foaming melts. The blowing agent decomposes under the influence of heat and releases gas, which then propels the foaming process. Shinko Wire Co., Amagasaki (Japan) has been using this foam production method since 1986 (Miyoshi et al. 2000). A Chinese company, Jiangsu Tianbo Light-Weight Materials in Nanjing, has been recently founded an Al foam processing plant that uses the same method. The method is shown schematically in Figure 2.3 (Banhart 2000a), in the first stage of the foam production about 1.5 wt.% calcium metal is added to the aluminum melt at 680 °C (Miyoshi et al. 2000). The melt is then stirred for several minutes during which the viscosity of the melt continuously increases by a factor of up to 5 owing to the formation of oxides, e.g. $CaAl_2O_4$, or intermetallics, which thicken the liquid metal. Calcium volume fraction and stirring time effects on the viscosity of an Al melt were shown in Figure 2.4 (Banhart 2000a). Upon reaching an optimum viscosity of the melt, titanium hydride is added in an amount typically 1.6 wt.%, which acts as a blowing agent according to the following reaction:

$$TiH_2 (s) \rightarrow Ti (s) + H_2 (g)$$
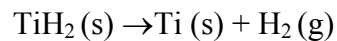
The melt starts to expand slowly and gradually fills the foaming vessel. The whole foaming process can take 15 minutes for a typical batch of about 0.6 m^3. After cooling the vessel below the melting point of the alloy, the liquid foam turns into solid aluminum foam and can be taken out of the mould for further processing.
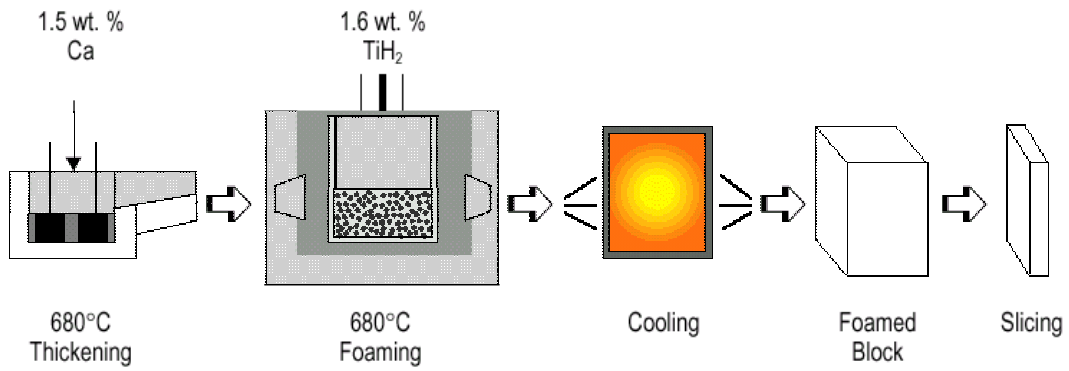
Figure 2.3. The process steps of aluminum foam forming by gas releasing agent, Alporas process.
(Source: Banhart 2000a)
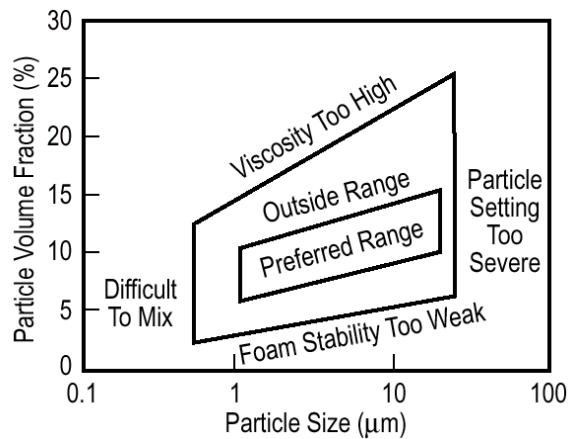
Figure 2.4. Effect of calcium (Ca) fraction and stirring time on the viscosity of Al melt.
(Source: Banhart 2000a)

Alporas™ foam manufactured in this way, has very uniform pore structure and do not require the addition of ceramic particles (Miyoshi et al. 2000), which makes the foam brittle. However, the method is more expensive than foaming melts by gas injection method owing to more complex processing equipments are needed. Nakamura et al. (2002) applied CaF_2 coated $CaCO_3$ as the foaming agent in the Alporas method. It was observed that carbonate foaming ensured smaller pores but similar densities as foaming with TiH_2.

2.2. Foaming of Powder Compacts

The process starts with the mixing of metal powders - elementary metal powders, alloy powders or metal powder blends - with a powdered blowing agent, after which the mix is compacted to yield a dense, semi-finished product (Baumgärtner et al. 2000) (Figure 2.5). Besides metal hydrides (e.g., TiH_2, ZrH), carbonates (e.g., calcium carbonate, potassium carbonate, sodium carbonate and sodium bicarbonate), hydrates (e.g., aluminum sulphate hydrate and aluminum hydroxide) or substances that evaporate quickly (e.g., mercury compounds or pulverized organic substances) can also be used as blowing agent.

Compaction techniques include uni-axial or isostatic compression, rod extrusion or powder rolling. Extrusion can be used to produce a bar or plate and helps to break the oxide films at the surfaces of the metal powders. Foaming agent decomposes and the material expands by the released gas forces during the heating process (350 ^{o}C– 450 ^{o}C) thus a highly porous structure is formed (Baumeister and Schrader 1992). The manufacturing process of the precursor has to be carried out very carefully because residual porosity or other defects will lead to poor results during further processing. The precursor material can be processed into sheets, rods, profiles, etc. by conventional techniques. The mixture of powders, metal powder and foaming agent, was cold-compacted and extruded to give solid metal material containing a dispersion of powdered foaming agent. When this solid was heated to the metal's melting temperature, the foaming agent decomposes to release gas into the molten metal, creating a metal foam. During this process, cooling the foam is a problem since after heating the precursor for foaming, the heat source could be turned off quickly. However, the metal would still be hot, and is prone to collapsing back into molten metal before it solidifies (Baumeister and Schrader 1992). Water-cooling or heating the foam only locally may avoid this problem, however the problem may become a significant challenge for the reliable foam production. The foam has a closed-cell structure with pore diameters in the range of 1 mm to 5 mm and the process is called baking.
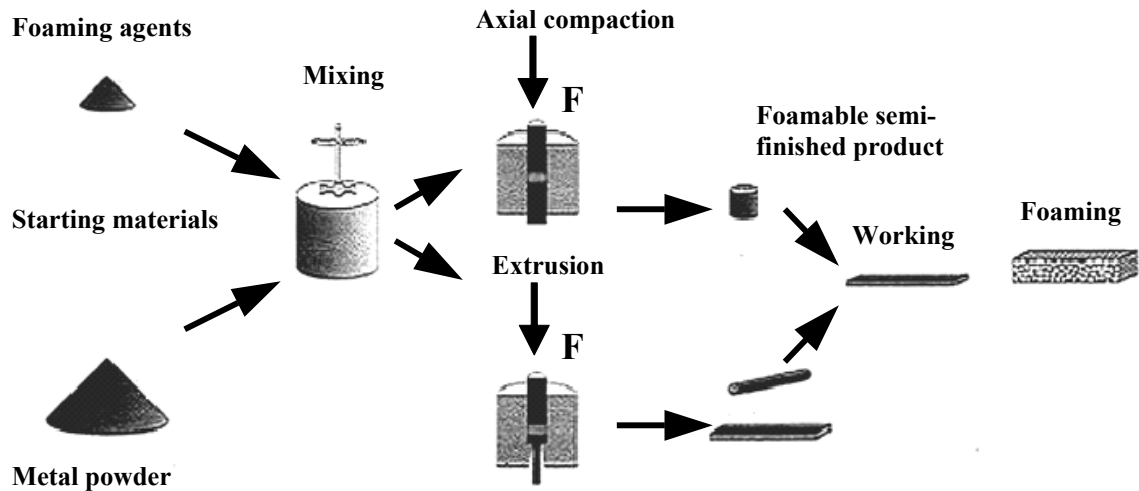
Figure 2.5. Foaming from powder compacts process.
(Source: Baumgärtner et al. 2000)

Another method of foaming of metallic melts applies investment-casting technique for open-cell foam production. Commercially known DUOCEL™ foam used in heat exchangers is manufactured by the investment casting. A ceramic replicate is produced using a polymeric foam precursor and then the liquid metals are impenetrate and replace the polymeric foam (Figure 2.6) WEB_1 (2005). A wide regular shape and uniformity of foam structure can be possible with this method. The process produces relatively small quantities of expensive, high-quality foams with reliable material properties. The porosities can be as high as 98%, with pore size between one and several millimeters. Any metal or alloy can be foamed, however, its widespread use is limited due to the complexity, cost and difficulty of scaling up the process WEB_2 (2003).

a) Preform Polymer ligaments   Casting slurry (sand)

b) Burnout
H_2O CO
Open channels
Mold material

c) Inflitrate
Pressure
Molten metal

d) Remove mold material
Metal ligaments
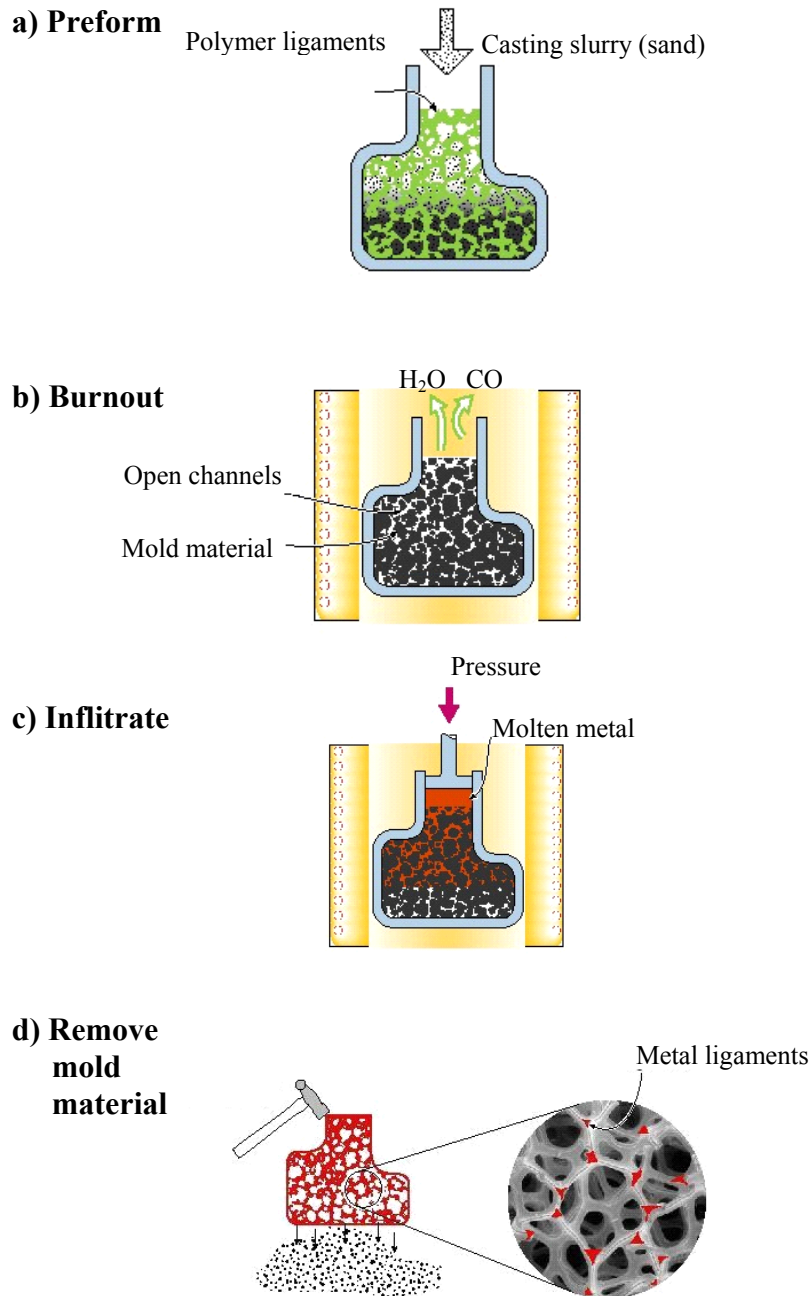
Figure 2.6. Investment casting method to manufacture open cell foams.
(Source: WEB_1, 2005)

2.2.1. Foaming of Ingots Containing Blowing Agents

In this process, melt processing is applied to produce a foamable precursor material. Titanium hydride particles are added into the liquid metal after which the melt is solidified. The resulting precursor can then be foamed in the same way as described

in previous section. To avoid premature hydrogen evolution during mixing, solidification has to be either rapid or the blowing agent has to be passivated to prevent it from releasing too much gas at this stage. One way is to use a die-casting machine (Gergely and Clyne 2000, Yu et al. 1998).

The powder hydride and the melt are injected into the die at the same time (Banhart 2000a). Achieving a homogeneous distribution of TiH_2 powders in the die is however difficult. Alternatively, TiH_2 powders can be added to a melt at comparatively slow stirring rates and subsequent cooling is provided such that they are subjected to a cycle of heat treatment that forms an oxide barrier layer on each hydride particle to delay their decomposition (Gergely and Clyne 2000). In order to obtain stable foams, 10-15% SiC particles are added into the melt. The process is called Formgrip, which is an acronym of "Foaming of Reinforced Metals by Gas Release in Precursors". Another version of Formgrip process is known as Foamcarp in which $CaCO_3$ is used to release CO_2 that is reduced to CO and oxidizes the surface of the cells, creating an oxide layer (Gergely et al. 2003).

CHAPTER 3

APPLICATIONS OF METALLIC FOAMS

Metallic foams have combinations of unique physicochemical and mechanical properties, which are not currently covered by other materials. They can potentially be used in many applications such as structural applications including energy absorption of impacts and explosions (Banhart and Baumeister 1998, Körner and Singer 2000). When used as cores of structural sandwich panels, they offer high stiffness in conjunction with high sound absorption capacity and low thermal conductivity. They can also be used as vibration absorbers and heat exchangers/interchargers. Therefore, one may classify metallic foams as the materials of multifunctionality. They are also recyclable and nontoxic, which make them more attractive materials. In Figure 3.1, some potential applications of the metal foams as function of open, partially open and closed pores are shown. While open cell foams are mostly preferred for functional applications, closed cell foams are suitable for structural applications (Banhart 2003).
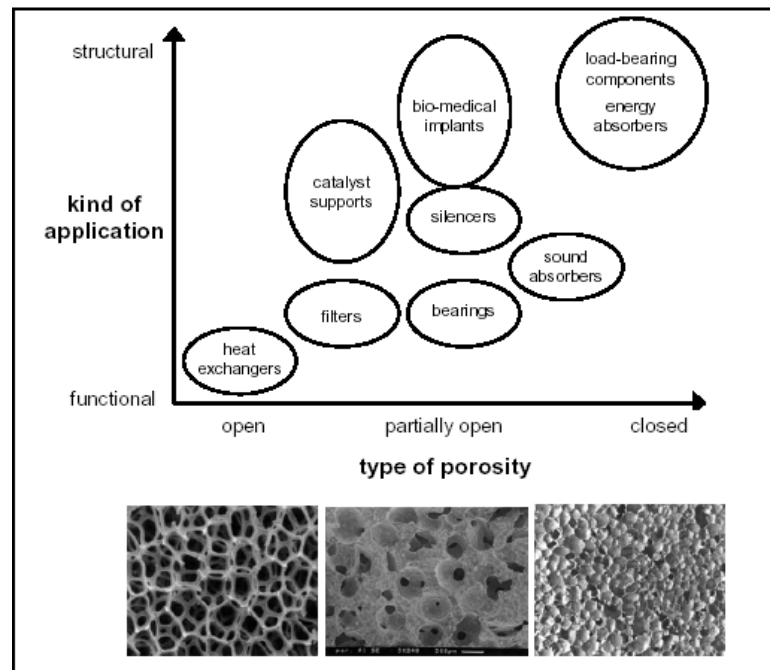
Figure 3.1. Application areas of cellular metals, grouped according to the degree of openness.

(Source: Banhart 2003)

3.1. Structural Applications

Aluminum foams are expected to find use in structural applications where weight is of particular concern, e.g. car bodies, doors and foot panels or portable electronic devices (Banhart 1999). Other potential applications include ships, buildings, aerospace industry and civil engineering WEB_3 (2005). Examples of the foam panels produced to be used in automobiles and ships are shown in Figures 3.2 (a) and (b) respectively (Baumeister 2000, Banhart 1999).

(a)   (b)
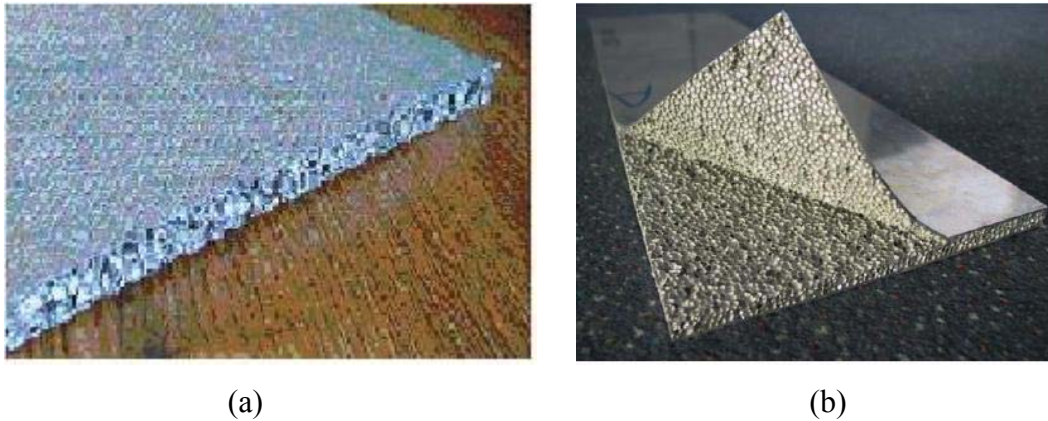
Figure 3.2. (a) Foam panel for automobile door and floor coatings, (b) Ship's wall Al foam panel coatings for noise attenuation produced by Karmann, Osnabrück.
(Source: Baumeister 2000, Banhart 1999)

Aluminum foams combine two important characteristics in their structure better than their own parent material. These are relatively high stiffness and lower density. It is important to note that, if only the direct strength is considered, foams often have a similar or worse performance than solid material of the same weight. The advantage of foams becomes apparent when bending stresses are considered as a function of weight (Banhart and Baumeister 1998). In lightweight constructions, Al foams can be used to optimize the weight-specific bending stiffness of engineering components. The bending stiffness of flat Al foam panels of a given weight, width and length, e.g., is approximately proportional to their thickness, and therefore inversely related to density. The mass distribution of cellular structures increases the overall moment of inertia of the material, giving a far higher specific bending stiffness and strength than for the

13

corresponding weight of bulk metal. Compared with solid metal components, structures produced using foam cores have been shown to be significantly lighter, while offering notably increased structural rigidity.

3.2. Heat Exchangers and Cooling Machines

Open-cell foams are conventionally used in heat exchangers and heat sinks (Banhart 2000b). In a typical heat exchanger, a fluid is circulated through the open-cell foam and alternatively, fluid could be circulated through the material, one surface of which was in contact with some power electronic device that required cooling. The high surface area, low flow resistivity and good thermal conductivity of foams make them more promising candidates for such applications than conventional heat sinks. As normally produced, aluminum foams tend to be sealed or nearly so on all surfaces which interface with the surface of the mould (Banhart 2000b). Owing to the open porosity, pressure drops can be also minimized. Examples of such applications are compact heat sinks for cooling of microelectronic devices with a high power dissipation density such as computer chips or power electronics. Another application field for open cellular materials is transpiration cooling.

3.3. Silencers

Components for dampening of sound, of pressure pulses or of mechanical vibrations are also common in industrial applications of powder metallurgy. Materials with a certain degree of open porosity can be tailored to damp some frequencies selectively while they allow passing others. Sudden pressure changes occurring, e.g. in compressors or pneumatic devices can be damped with foams. Materials such as the investment cast foams or the foams made by deposition could replace such traditional elements for reasons of cost and effectivity (Eisenmann 1998).

3.4. Acoustic Applications

Closed-cell Aluminum foams are poor sound absorbers but both opened and semi-opened aluminum foams are good sound absorbers and they are currently used for

noise reduction (Ashby et al. 2000, Lu et al. 1999). However, closed-cell aluminum foams can have good sound absorption capacity after some processes such as hole drilling, rolling and compression. In order to maintain the best absorption values of the chosen materials, the air channels should all be open to the surface so that sound waves can propagate into the material. If pores are sealed, as in closed-cell foam, the material is generally a poor absorber (Ashby et al. 2000). Sound absorption materials control airborne noise by reducing the reflection of sound from the surface boundaries thus reducing the overall noise levels. Sound is attenuated by vibration and friction losses by the repeated reflections within the cell structure where full absorption is possible (Eisenmann 1998). Sound absorption properties of foams however can be varied such that foams can only be used to eliminate certain frequencies. Al foams also can be used in a wide variety of noise control treatments such as machinery enclosures, plant machinery, walls, in automobiles for engine, tire, door noise and sides of roads to reduce traffic noise (Urban et al. 2004, Biermann et al. 2004). Al foam is normally employed as an internal lining to machinery guards or enclosures. The damping capacity of foamed aluminum has been shown to be an order of magnitude higher than that of the bulk metal (Eisenmann 1998).

3.5. Flame Arresters

Cellular metals with high thermal conductivities of the cell wall material can be used to stop flame propagation in combustible gases. Open cell foams have been shown to be capable of arresting flames even when they were traveling at velocities up to 550 m/s WEB_4 (2005). In practice, long runs of pipes transporting combustible gases are protected close to possible sources of ignition so that, if ignition does occur, the flame can not accelerate to high velocities WEB_5 (2004). They can also be used in blast protection applications (Eisenmann 1998).

3.6. Energy Absorption Applications

Metallic foams have excellent energy absorbing properties. Therefore, they are preferred materials as the filler material in crash absorbing members (Figure 3.3) (Banhart 2003). The foam filler supports the tube wall, causing buckling of the wall at a

15

higher load (interaction effect) (Hanssen et al. 2000). Consequently, the mass specific energy absorption of the tube increases. In addition, the initial deformation resistance peak of the tube is reduced as compared to an empty tube of same weight. This second phenomenon is important because a lower deformation resistance translates into a lower acceleration on the occupants of a vehicle. The graph below shows both the higher overall load and the relatively reduced initial peak load measured during crushing. The foam filled crush tube with the same energy absorption capability as the empty tube can be considerably lighter (Figure 3.4) (Hanssen et al. 2000).

Figure 3.3. Examples of foam filled tubes.
(Source: Banhart 2003)
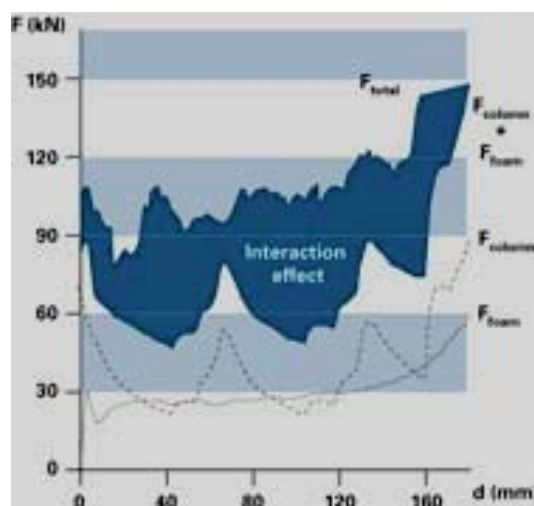
Figure 3.4. Load-displacement curve showing interaction effect in foam filled tube.
(Source: Hanssen et al. 2000)

3.7. Corrosion-resistant Applications

Aluminum has good resistance to oxidation and many forms of chemical attack. Open-cell foams with small pore sizes can thus be used as high-temperature or chemically resistant filter materials. Liquid fuel containers could be part-filled with open-cell foams, so that in the event of breakage, flammable materials would at worst seep out gradually and burn on the surface of a block, rather than spilling over a large area before catching fire.

3.8. Automotive Applications of Aluminum Foams

Another application makes use of the beneficial properties of Al foam inside a dense aluminum shell both during manufacture and in use after. These types of foams are manufactured first by Alulight. The part has a dense outer skin. Therefore, it can be used as core in low-pressure die-casting during which a composite consisting of a cast outer surface and a lightweight inner core is formed (Leitlmeier et al. 2002, Fuganti et al. 2000). Such composites have advantageous service properties such as higher stiffness and improved damping compared to the empty hollow part while its weight is only marginally higher. LKR (Austria) and the German carmaker BMW have jointly designed an engine-mounting bracket based on such composites (Figure 3.5) (Banhart 2003). The produced parts show no noticeable infiltration of the core itself by the melt during casting. It can be loaded with the high weight of a car engine and absorbs mechanical vibrations by internal dissipation into thermal energy. Stiffness is enhanced and, as fracture toughness of such composites is high, these parts also increase safety in crash situations. In addition, aluminum foams are going to be used for sound attenuators in automobiles as foot panels, doors, back of the power-train (dash panel) sections (Figure 3.6). In a vehicle, interior noise was caused by several parts of the car body, such as engines, exhaust system, suspension, tyres, etc. and interior thermal problems caused by power-train, exhaust system, body panel, etc., are the main problems that the automobile manufacturers, designers and OEM manufacturers faced for several years (Fernández and Wittig). The major noise and heat sources, in their order of significance, in the vehicle are:

> ➤ Engines - crankcase, oil sump, cylinder head

- ➢ Tappet covers, engine mounts besides combustion
- ➢ Exhaust system, Intake system
- ➢ Transmission
- ➢ Fan and cooling system
- ➢ Tyres
- ➢ All the body panels including that of bonnet.
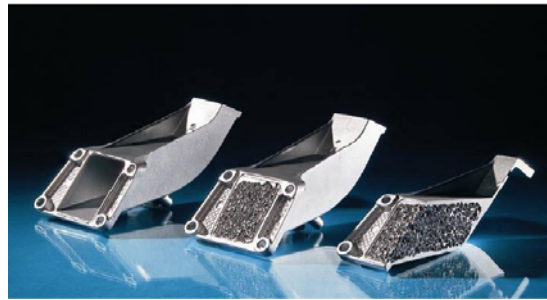
Figure 3.5. Prototype of a BMW engine-mounting bracket manufactured by LKR Ranshofen. (From left to right: empty casting, entire composite part consisting of foam core and cast shell, section through composite part). (Source: Banhart 2003)
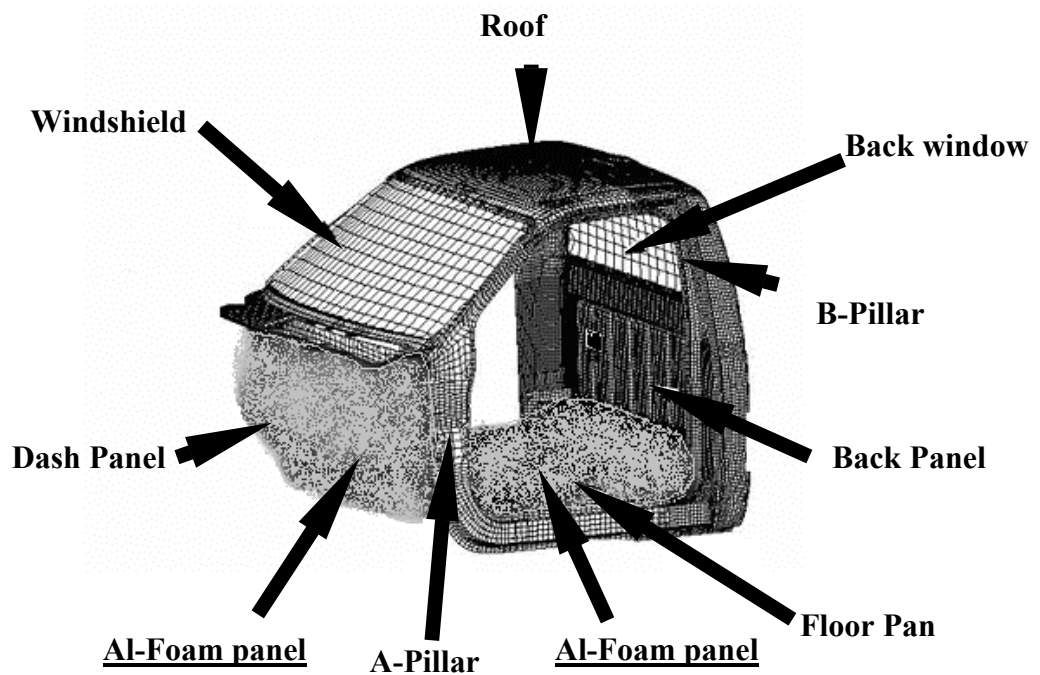
Figure 3.6. Probable application parts of aluminum foams in a car cab.

CHAPTER 4

EFFECTIVE THERMAL CONDUCTIVITY MEASUREMENTS OF POROUS MEDIA

4.1. Heat Conduction

Heat transfer by conduction may be defined as the flow of heat from a hot part of a body to a cooler part of the same body, or from one body to another in physical contact with it, without transfer of matter. The ability of a substance to conduct heat is measured by its thermal conductivity (Holman 2002, Kakaç 1998). The rate at which heat is transferred in a body (**Q**) is proportional to the cross-sectional area, **A**, of the body, and the temperature gradient (**dT/dx**) along the direction of heat flow (Figure 4.1).
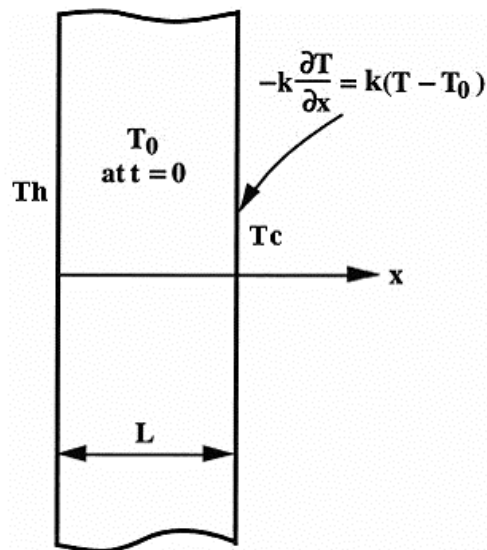
Figure 4.1. Heat flow along a uniform insulated bar.
(Source: Holman 2002)

The factor k, shown in Figure 4.1, is called the thermal conductivity; it is a characteristic property of the material, which the heat is flowing through and it varies with temperature:

$$k = - \frac{QL}{A\Delta T} \quad \text{(W/m·K)} \quad (4.1)$$

where L is the characteristic length of the solid material in the direction of heat flow, and ΔT is the temperature difference between the ends of the body. The thermal conductivity k can also be defined as the heat flux Q/A (the amount of heat flowing across a unit area per unit time) induced by the temperature gradient dT/dx. In one-dimensional heat flow it is:

$$q' = \frac{Q}{A} = - \frac{kdT}{dx} \quad \text{(W/m}^2\text{)} \quad (4.2)$$

The temperature gradient term in Equation 4.2 can be defined as the change of temperature per unit distance along the bar at any position and will be:

$$\frac{dT}{dx} = \frac{T_{cold} - T_{hot}}{\Delta x} \quad (4.3)$$

The units of thermal conductivity are $J.s^{-1}.m^{-1}.K^{-1}$, or $W\ m^{-1}\ K^{-1}$ (W/m·K), or Btu/h·ft· °F, if Equation 4.2 is to be dimensionally correct. Conduction can also take place from one body to another, provided the two bodies are in contact, and a temperature difference exists between them. In a solid, the particles (atoms or molecules) are close to one another. If heat is applied to one end of a bar of the material, the particles that are heated will vibrate more energetically. The energy of these vibrations is transmitted to the neighboring particles, causing them to vibrate.

Materials differ widely in their ability to conduct heat. There are good thermal conductors such as metals and on the other hand, wood, glass, and various plastics are very poor heat conductors. Liquids and gases are also poor conductors of heat. The substances, which have air trapped in their structures, are extremely poor conductors

and are classified as insulating materials. The thermal conductivities of various substances are listed in Table 4.1 (Lienhard IV and Lienhard V 2001).

Table 4.1. Thermal conductivities of various substances at room temperature.
(Source: Lienhard IV and Lienhard V 2001)

Increasing (k)

Substances	Thermal Conductivity W/m·K
Copper	391
Aluminum	236-240
Steel (0.5 % carbon)	52-55
Ice	2.215
Concrete (sand & gravel)	1.8
Glass (plate)	1.3
Water	0.61
Wood	0.16-0.4
Polystyrene	0.1-0.16
Glass wool	0.04
Air	0.026

4.2. Effective Thermal Conductivity of Foams

In aluminum foams since the heat conduction occurs through the solid and fluid phase, the thermal conductivity is called effective thermal conductivity. Therefore, the effective thermal conductivity is a property showing the ability of a closed-cell foam to conduct the heat through the gas (air) and solid (aluminum) phase with no flow of fluid (Hegman and Babcsán 2005). The effective thermal conductivity (ETC) of foams can be calculated by considering four different contributions: (1) conduction through the solid, (2) conduction through gas, (3) convection within the cells, (4) radiation through the cell walls and across the cell voids (Amjad 2001). Conduction is the main mode of heat transfer when surfaces of two materials with different temperatures are in close contact. The effective thermal conductivity varies with the material structure (foam density, pore

size, void fraction) and with the internal environment. In addition, conduction depends strongly on the cross sectional area A enabling the thermal flow rate through the specimen. In foamed aluminum, only a small part of the cross section (pore walls) is metallic with the thermal conductivity given by the base alloy. The rest are the pores filled with gas that has a much lower thermal conductivity than aluminum. The density of the foam describes the ratio of walls to pores. Therefore, the cellular structure provides much lower thermal conductivity than any bulk material. Convection is the main mode of heat transfer between a surface and a moving fluid at different temperatures. In foams, convection becomes significant when the cell size more than 10 mm or so in diameter, because the fluid particles inside the cell find space to move and convect heat (Hegman and Babcsán 2005). Since currently used aluminum foams have cell sizes between 0.5 mm and 2 mm ranges, hence, the contribution of the convection is negligible. Radiation is the transfer of energy through electromagnetic waves (by means of wave motion through space) when there is no conveying medium present (Holman 2002). Stefan's Law describes the heat flux passing by radiation from one surface to one at lower temperature with vacuum in between them (Holman 2002);

$$Q = \sigma_{sb}\, T^4 \quad \text{(W)} \tag{4.4}$$

where σ_{sb} is Stefan's constant (5.67 x 10^{-8} W/m$^2\cdot$K^4) and T is the temperature difference. The radiation effect is small, especially at low temperatures (below 100 °C), compared to the conduction and convection effects, and can be safely ignored (Hegman and Babcsán 2005).

4.2.1. Combination of Heat Transfer

In a porous system, many factors should be considered to calculate the heat flow values. The combination of conduction through the solid phase, conduction through the enclosed gas usually gives a complex heat flow, which is described by an effective thermal conductivity. These values can be added to determine the effective thermal conduction by a simple addition:

$$k^* = k_s + k_f + k_c + k_r \tag{4.5}$$

where k_s is the contribution of thermal conductivity from conduction through the solid, k_f is that from the fluid, k_c is the thermal conductivity due to convective processes and k_r is the contribution from radiation. In metal foams, the gas contained in the cells have a low weight, hence the specific heat of the foam is nearly equal to the solid from which it is made. In addition, heat transfer increases with cell size, this is because radiation is reflected less often in foams with large cells (Gibson and Ashby 1997). Besides cell size, porosity is an important measurable parameter for thermal conduction, which can be calculated by the following simple formula:

$$\phi = \frac{(V_{foam} - \frac{m}{\rho})}{V} = 1 - \frac{\rho*}{\rho} \qquad (4.6)$$

where V is the volume of the foam material, ρ and $\rho*$ are the solid and foam density, respectively. Other factors like the fraction of open cells, also affect heat transfer but to a lesser extent. Temperature is another factor, which can affect effective thermal conductivity. As the temperature decreases, effective thermal conductivity decreases through solids and gases. Hence, the heat transfer in foams decreases steeply with decreasing temperature (Hegman and Babcsán 2005).

4.3. Effective Thermal Conductivity Predictions of Aluminum Foams

Maxwell (1873) and Lord Rayleigh (1892) conducted the first investigation for the effective thermal conductivity of porous media. Tien and Vafai (1982) developed a model by defining the effective thermal conductivity in the volume averaged homogeneous energy equation. After that Hunt and Tien (1988) used the Empirical stagnant conduction model for predicting the effective thermal conductivity.. First approach for determining the effective thermal conductivity of a fluid filled porous media is shown by the following equation:

$$k_e = k_f + (1 - \phi)k_s \qquad (4.7)$$

where k_e is the effective thermal conductivity, k_f is the thermal conductivity of the fluid phase, k_s is the thermal conductivity of the solid phase and ϕ is the porosity of the

system and it is defined as the total void volume divided by the total volume of the foam also porosity is the fraction of the area that will conduct heat due to gas conduction (Equation 4.6). Equation 4.7 can not predict accurately the effective thermal conductivity of a porous media, but it gives the maximum value for the effective thermal conductivity. There are several approaches that could describe the effective thermal conductivity in terms of two limiting cases: thermal conduction in parallel and series arrangements (Figure 4.2), which are given by the following equations:

$$k_{parallel} = \phi \, k_f + (1 - \phi) k_s \tag{4.8}$$

$$k_{series} = \frac{k_s \, k_f}{\phi \, k_s + (1 - \phi) \, k_f} \tag{4.9}$$

These arrangements can be explained by the following figures:
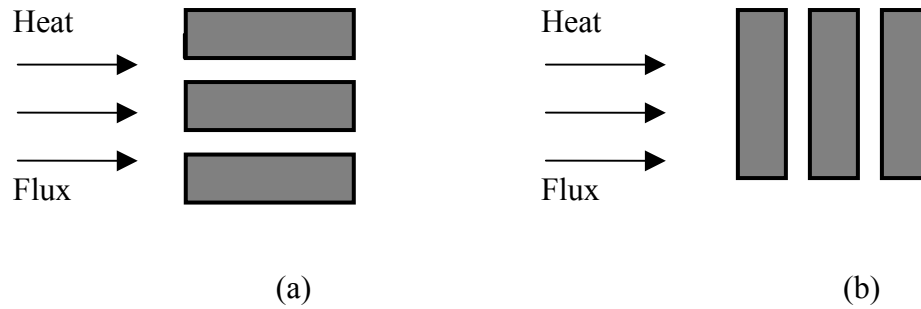
Figure 4.2. Configuration of the resistors in a (a) parallel and (b) series systems.

The accurate value of the k_e lies between the equations given above. The term $(1 - \phi)$ is the fraction of the area that will conduct heat due to solid conduction. Another approach assumes the combined conduction thermal conductivity can be calculated by a superposition of Equations 4.8 and 4.9 as:

$$k = A k_{parallel} + (1 - A) \, k_{series} \tag{4.10}$$

where A is the fraction of heat transfer in parallel mode and $(1-A)$ is the fraction of heat transfer in series mode (Daryabeigi 1999). Bhattacharya et al. (1999) applied following

empirical combined conduction effective thermal conductivity equations by taking the square root of the sum of the squares of the parallel and series arrangements as:

$$k_e = \sqrt{[A\,(k_{parallel})^2 + (1-A)\,(k_{series})^2]} \qquad (4.11)$$

Moreover, Bhattacharya et al. (2002) provided analytical and experimental results for the effective thermal conductivity of high porosity metal foams. Their analytical model represented the foam by a two-dimensional array of hexagonal cells and shown in Figure 4.3 (Amjad 2001). In their study, the porosity and the pore density were used to describe the porous media. They used air and water as the fluid media to validate the analytical solutions of experimental data with aluminum foams. They assumed that effective thermal conductivity could be expressed by the following correlation of the both series and parallel arrangements:

$$k_e = [A\,(\phi\,k_f + (1-\phi)k_s)] + \dfrac{1-A}{\left(\dfrac{\phi}{k_f} + \dfrac{1-\phi}{k_s}\right)} \qquad (4.12)$$

This above formula satisfied both the limits when $\phi = 0$ for solid and $\phi = 1$ for fluid. The best fit for all data was found for $A = 0.35$.

Singh and Kasana (2004) applied a resistor model to predict the effective thermal conductivity of foams. The equation of the model is:

$$k_e = k_{parallel}{}^{A}\cdot k_{series}{}^{(1-A)} \qquad A \geq 0,\ 0 \leq A \leq 1 \qquad (4.13)$$

where A^{th} fraction of the material is oriented in the direction of heat flow and remaining $(1-A)^{th}$ fraction is oriented in the perpendicular direction. When Equation 4.13 was solved for A in terms of $k_{parallel}$, k_{series}, k_e and the solution is:

$$A = \dfrac{\ln(\phi\dfrac{k_e}{k_f} + (1-\phi)\dfrac{k_e}{k_s})}{\ln(1 + \phi(1-\phi)(\dfrac{k_s}{k_f} + \dfrac{k_f}{k_s} - 2))} \qquad (4.14)$$

They used a curve fitting technique and found that the expression:

$$A = C_1 + C_2 \ln(\phi \frac{k_s}{k_f})$$ (4.15)

After using several combinations they fitted the curve in $C_1 = 0.3031$ and $C_2 = 0.0623$. However, it was observed from their experiments that Equation 4.15 did not give the results of a real system. Therefore, they modified a constant C for appropriate A values:

$$A = C(0.3031 + 0.0623 \ln(\phi \frac{k_s}{k_f}))$$ (4.16)

where C is a constant and the average values of C were found 0.9683 and 1.0647 for aluminum-air and aluminum-water, respectively. Well agreements between experimental data and theoretical results were found and they compared their results with the Boomsma's and Bhattachyra's models.
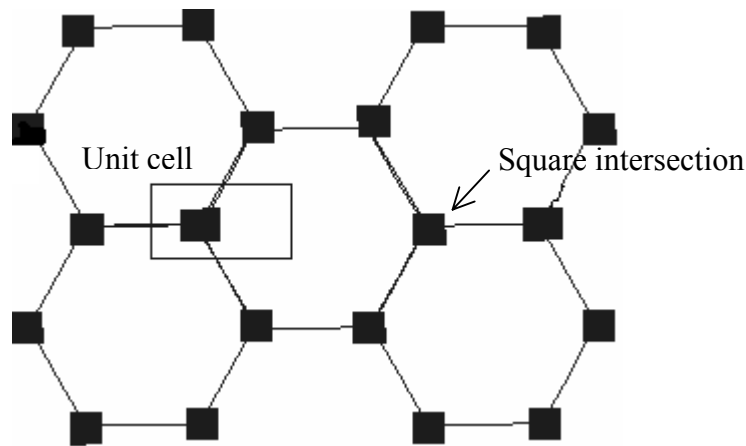
Figure 4.3. The hexagonal structure of the metal foam matrix.
(Source: Amjad 2001)

Zhao et al. (2004) studied the dependence of the effective thermal conductivity on the temperature in metal foams. They measured the effective thermal conductivity of five FeCrAlY foam samples with different pore sizes and relative densities by using a guarded-hot-plate apparatus under both vacuum and atmospheric conditions. Their

results showed that the effective thermal conductivity increased rapidly as the temperature increased, particularly in the higher temperature range (500-800 K) where the thermal radiation dominated the transport. Their results showed that the contribution of the heat transfer by natural convection was also significant at that temperature ranges. They observed that the effective thermal conductivity increased as the pore size or relative density increased. In addition, relative density had a great effect on the natural convection in the metal foam.

Writz (1997) developed a semi-empirical model for the combined conduction and convection heat transfer in a thin porous wall. The model assumed a one-dimensional conduction in the porous matrix and a one-dimensional flow of the coolant through the foam wall. They found that for the same volume of the heat exchanger, the porous matrix provided approximately 1.5 times more heat transfer surface than the offset strip fin array.

N.Babcsan et al. (2003) measured the effective thermal conductivity of closed cell Alporas foams with different density and cell size distributions. They chose the comparative method to determine the effective thermal conductivity of the samples as a function of temperature between 30 and 500 ^{o}C. The focus of their study was on the determinations of the magnitude of the contributions to heat transfer in metallic foams through solid conduction, thermal radiation, gaseous conduction and convection.

Boomsma et al. (2003) investigated the heat transfer properties of open-cell aluminum foam for the electronic cooling applications. Their foam samples were compressed at different deformation ratios. It was shown that the foam manifested a significant improvement in the efficiency to exchange heat after compression. Boomsma and Poulikakos (2001) investigated the geometrical effective thermal conductivity of saturated porous metal foam based on idealized three-dimensional basic geometry of a foam composed of tetrakaidecahedron cells as shown in Figure 4.4 (a). In the unit cell (Figure 4.4(b)) model L_A, L_B, L_C and L_D are the convenient layers with a length of a, r/2, 0.707L-r and r/2, respectively.

(a)	(b)
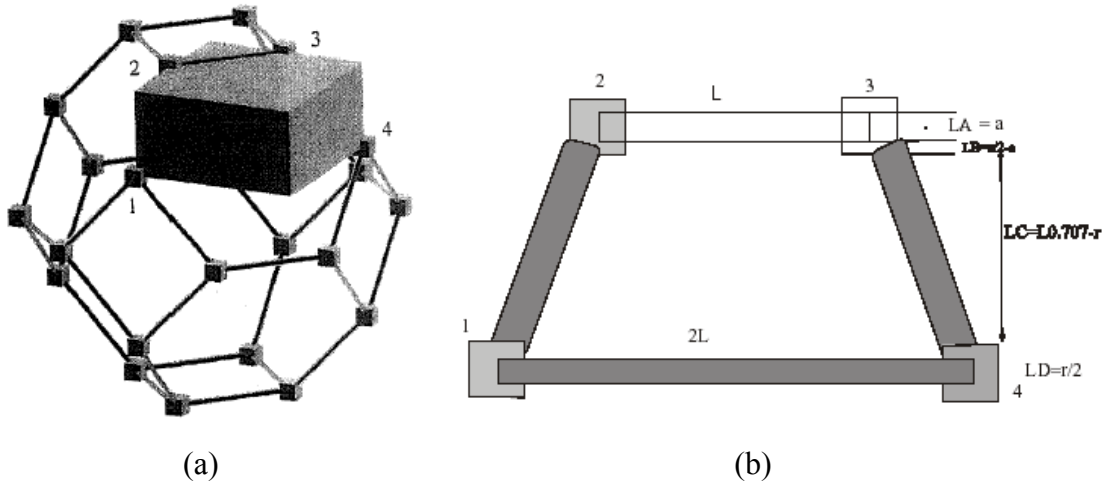
Figure 4.4. (a) Tetrakaidecahedron cell model and (b) the unit cell located in a single cell.

(Source: Boomsma and Poulikakos 2001)

For the model the effective thermal conductivity was formulated as:

$$k_e = \frac{\sqrt{2}}{2[R_A + R_B + R_C + R_D]} \qquad (4.17)$$

where R_A, R_B, R_C and R_D (W^{-1}m·K) are the simplifying quantities for each unit cell subsection and can be expressed by the following equations:

$$R_A = \frac{4d}{[\{2e^2 + \pi d(1-e)\}k_s + \{4 - 2e^2 - \pi d(1-e)\}k_f]}, \qquad (4.18)$$

$$R_B = \frac{(e-2d)^2}{[(e-2d)e^2 k_s + \{2e - 4d - (e-2d)e^2\}k_f]}, \qquad (4.19)$$

$$R_C = \frac{(\sqrt{2} - 2e)^2}{[\{2\pi d^2(1 - 2e\sqrt{2})k_s\} + 2\{\sqrt{2} - 2e - \pi d^2(1 - 2e\sqrt{2})\}k_f]}, \qquad (4.20)$$

$$R_D = \frac{2e}{[e^2 k_s + (4 - e^2)k_f]} \qquad (4.21)$$

28

where *d* is the dimensionless foam ligament radius and it can be expressed by the following equation:

$$d = \sqrt{\frac{\sqrt{2}(2 - (5/8)e^3\sqrt{2} - 2\phi)}{\pi(3 - 4e\sqrt{2} - e)}} \qquad (4.22)$$

where e is the dimensionless cubic node length and its values is 0.339. The model showed that significant improvements in the overall effective thermal conductivity of a metal foam could be possible through the increasing the thermal conductivity of the solid phase and manipulation of the foam solid structure at the manufacturing phase, since the solid phase appeared to govern the effective thermal conductivity value even at a very high porosity. They also predicted that the effective thermal conductivity of the open-cell foam, having 95% porosity, was 3.82 $W.m^{-1}.k^{-1}$ and with use of air as the saturated fluid under vacuum, the effective thermal conductivity increased to a value of 3.85 $W.m^{-1}.k^{-1}$ and with water to 4.69 $W.m^{-1}.k^{-1}$. Hence, this shows that the overall effective thermal conductivity of the foam was strongly affected by the heat conductivity of the solid phase, even in foams with high porosity level.

Gibson and Ashby (1997) described the solid thermal conductivity by multiplying thermal conductivity of the bulk material by the solid conduction efficiency factor, ζ, which permits for the tortuous structure for conduction through the cell walls.

$$k_s = \zeta \cdot k_{bulk} \qquad (4.23)$$

Calmidi and Mahajan (1999) developed a single relation for aluminum foams by combining Equations 4.8 and 4.23:

$$k_{cond} = \phi \, k_f + (1-\phi)^m \cdot D \cdot k_{bulk} \qquad (4.24)$$

They found that in Equation 4.24, D = 0.181 and m= 0.763 values showed a perfect matching to their experimental results. Daryabeigi (1999), Sullines and Daryabeigi (2001) conducted their study with Equation 4.24 and they found a perfect match between experimental results and theoretical results for a fibrous insulation when D = 1 and m = 3.

CHAPTER 5

SOUND ABSORPTION IN POROUS MEDIA

5.1. Nature of Sound

Sound is the vibration or wave of air molecules produced when an object moves or vibrates through a medium from one location to another. A wave can be described as a disturbance that travels through a medium, transporting energy from one location to another location. The medium is simply the material through which the disturbance is moving. When an object moves or vibrates, the air molecules around the object also vibrate, producing sound. During movement, air particles bump into each other and produce a sound wave. Sound can travel through any medium except vacuum.

Compressive (longitudinal) waves have a frequency that is within the audible spectrum and where particles of the medium are temporary displaced in a direction parallel to energy transport (Figure 5.1) and then return to their original position (Ziomek 1995, Pain 1993). In transverse wave, particles of the medium are temporary displaced in a direction normal to energy transport (Figure 5.2) (French 1971).
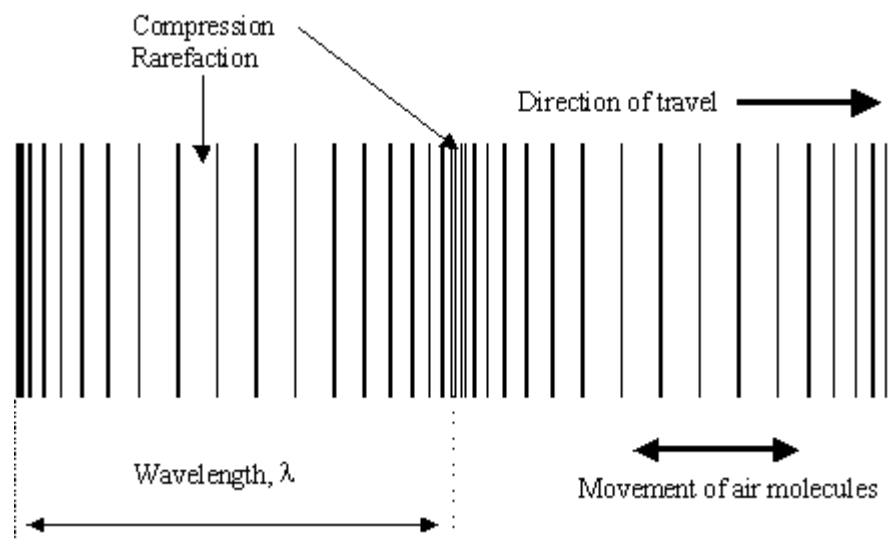
Figure 5.1. Schematic view of longitudinal waves.
(Source: Ziomek 1995)
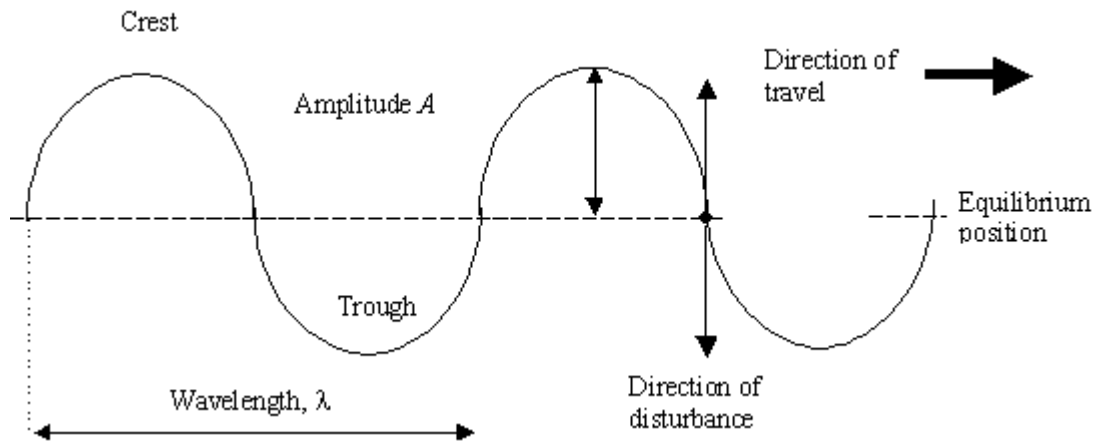
Figure 5.2. Schematic view of transverse waves.
(Source: French 1971)

The vibrations can also squeeze the air molecules together very hard or very gently. The squeezing is called amplitude and represented as tall or short waves. The more pushed an object to make it vibrate, the larger the vibrations and the louder the sound, or the greater the amplitude. Sound waves with the same frequency can have different amplitudes. The number of pressure variations per second is called the frequency of sound (f), which is measured in cycles per second, called Hertz (Hz),

$$f = v/\lambda \quad \text{(Hz)} \tag{5.1}$$

where v (m/s) is the wave speed and λ (m) is the wavelength. Wavelength is defined as the distance a pure tone wave travels during a full period (Figure 5.2). A sound that has only one frequency is known as a pure tone. The wavelength of a pure tone is equal to the speed of sound divided by the frequency of the pure tone. A young person with normal hearing can perceive sound in the frequency range of roughly 20 Hz to 20,000 Hz, defined as the normal audible frequency range (Raju 2003). The frequency of sound depends on how fast they vibrate. The frequency of a sound wave is called pitch. High frequency sounds are said to be high-pitched or just high and low frequency sounds are said to be low-pitched or just low. Pure tones are seldom encountered in practical applications as most sounds are made up of different frequencies. The most of industrial noise will consist of a wide mixture of frequencies known as broadband noise. The

reciprocal of the frequency of a pure tone is called the period (T) and defined as the time required for one complete cycle of the sinusoidal tone;

$$T = 1/f \quad \text{(s)} \tag{5.2}$$

The important property of a sound wave is that a sound wave can be reflected, refracted (or bent), and absorbed in a way same as the light waves. Sounds with frequencies above the range of human hearing are called ultrasound. Sounds with frequencies below the range of human hearing are called infrasound (Raju 2003). Sound levels are described on a logarithmic scale in units called decibels (dB). They are described logarithmically because it compresses the large range of typical sound pressures into a smaller, more practical scale, which incidentally also more closely parallels the human ear's ability to judge the relative loudness of sounds according to the ratio of their pressure.

Sound power level and sound pressure level are typically expressed in terms of decibels. The decibel represents a relative measurement or ratio. The sound power level (L_w or SWL) is the total sound power *(W)* radiated from a source with respect to a reference power of $W_{ref} = 10^{-12}$ W. Sound power level can be calculated using the following formula:

$$L_W = 10 \log_{10}(W/W_{ref}) \quad \text{(dB)} \tag{5.3}$$

A variation in pressure above and below the atmospheric pressure is called sound pressure and is measured in units of Pascal (Pa). The quantity most often used to measure the strength of a sound wave is the sound pressure level (L_p or SPL) measured with respect to a standard reference pressure of $p_{ref} = 2 \times 10^{-5}$ Pa. The sound pressure level can be calculated using the following formula:

$$L_p = 20\log_{10}(p/p_{ref}) \quad \text{(dB)} \tag{5.4}$$

where p is the mean-square sound pressure and p_{ref} is the reference sound pressure. In practice, it is more convenient to use the SPL scale as the most of acoustic measurements. While both sound power levels and sound pressure levels are expressed in decibels, the reference standard for each of them is different. More importantly, the

sound power level is the total acoustic energy output of a noise source independent of environment. Sound pressure levels are dependent on environmental factors such as the distance from the source, the presence of reflective surfaces and other characteristics of the room/building/area hosting the source. Actual sound pressure levels will always be higher than sound power levels (Ziomek 1995). The sound pressure is also additive, for instance, if the sound pressure is 74 dBA in a car cab, the sound pressure of power-train at 70 dBA will raise the noise level. Thus, any noise eliminated will reduce the overall noise level in the car's cab. Therefore, the automotive manufacturers started to use metal foam panels in car cabs for several parts to reduce unwanted sound (noise).

The speed of sound is the rate at which a sound wave propagates through a given medium. The equation for the speed of sound in air is:

$$v = 20.05 \sqrt{T} \quad \text{(m/s)} \tag{5.5}$$

where T is the absolute temperature of air in degrees Kelvin. At room temperature and standard atmospheric pressure, the speed of sound in air is 343 m/s. The speed at which sound travels through a medium depends on the elasticity, density and temperature of the medium. The speed of sound also depends upon the type of medium and its state. Table 5.1 lists the equations used to predict the speed of sound in gases, liquids and solids (Ziomek 1995).

Table 5.1. Equations of speed of sound in different media.
(Source: Ziomek 1995)

Gases	Liquids	Solids
$v = \dfrac{\sqrt{B}}{\rho} = \dfrac{\sqrt{\gamma P}}{\rho} = \dfrac{\sqrt{\gamma k T}}{m}$	$v = \dfrac{\sqrt{B}}{\rho}$	$v = \dfrac{\sqrt{Y}}{\rho}$

5.2. Sound Absorption

When the sound travels through a medium, its intensity diminishes with distance. In idealized materials, sound pressure is merely reduced by the spreading of the wave. In natural materials, however, the sound is further weakened by scattering and absorption. The combined effect of scattering and absorption is called attenuation (Brown 2000). The combination of fluctuations in pressure and velocity can be used to form a measure of sound power. Sound-absorbing materials such as absorbent ceiling panels, carpeting on the floor, and drapes or special absorbent wall coverings, are commonly used in industry to reduce noise for which the sound waves are reflected, absorbed and transmitted when they hit a hard surface (Figure 5.3). Three terms can define and evaluate sound absorption. These are the sound absorption coefficient, sabine, and noise reduction coefficient. The sound absorption coefficient is a measure of the proportion of the sound striking a surface, which is absorbed by that surface, and is usually given for a particular frequency. Thus, a surface which would absorb 100% of the incident sound would have a sound absorption coefficient of 1.00, while a surface which absorbs 35% of the sound, and reflects 65% of it, would have a sound absorption coefficient of 0.35. The sound absorption coefficients of commonly used materials are listed in table 5.2 (Brown 2000).

Table 5.2. Sound absorption coefficient of some selected materials measured
at 500 Hz
(Source: Brown 2000).

Material	Sound absorption coefficient, (α)
Plaster walls	0.01 – 0.03
Unpainted brickwork	0.02 – 0.05
Painted brickwork	0.01 – 0.02
3 mm plywood panel	0.01 – 0.02
6 mm porous rubber sheet	0.1 – 0.2
12 mm fiberboard on battens	0.3 – 0.4
25 mm wood wool cement on battens	0.6 – 0.07
50 mm slag wool or glass silk	0.8 – 0.9
Hardwood	0.3
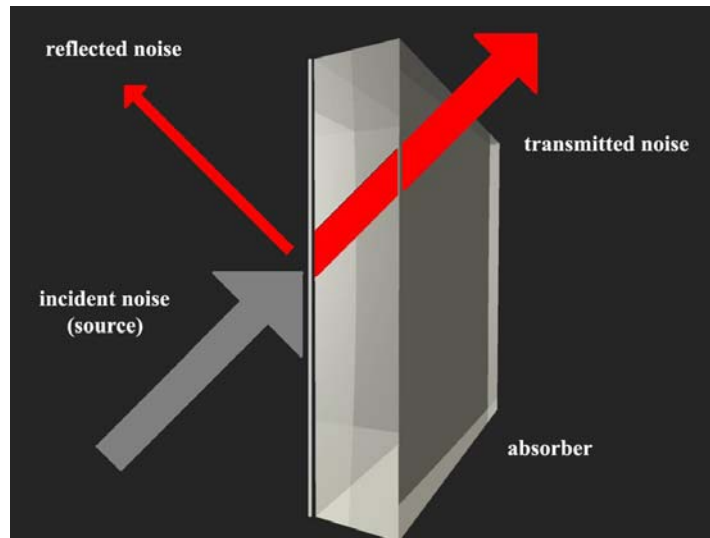
Figure 5.3. Sound absorption and reflection of a material.

A Sabine of absorption is defined as the amount of sound absorbed by one square foot of surface having a sound absorption coefficient of 1.00. The noise reduction coefficient is the average of the sound absorption coefficient at 250, 500, 1000 and 2000 cps (cycle per steps) in octave steps (Lam 1995, Beranek and Ver 1992).

In evaluating materials for their ability to absorb sound energy, its ability to absorb sound is usually provided in the form of an absorption coefficient $(\alpha.)$.When sound energy is incident upon a material surface, some of the vibration energy is transferred to the material and becomes dissipated in the form of heat and the energy is said to be absorbed. This can happen in many ways: a) by viscous losses as the pressure wave pumps air in and out of cavities in the absorber, b) by thermal-elastic damping, c) by Helmholtz-type resonators, d) by vortex shedding from sharp edges, e) by direct mechanical damping in the material itself. The amount of energy, which is absorbed per unit surface area is dependent upon the type of material and is characterized by an absorption coefficient (Lu et al. 1999). Materials which are dense and have smooth surfaces, such as glass, have small absorption coefficient, whereas porous-type materials, such as glass wool, that contain networks of interconnected cavities tend to scatter the sound energy and tend to trap it. Therefore, there is greater interaction at the surface of such materials and more opportunities during these scattering reflections for the sound wave to lose energy to the material. Consequently, these materials possess relatively larger sound absorption coefficients. The absorption of sound is dependent on

35

the vibration frequency of the air molecules and so, in general, there is greater absorption of sound at higher frequencies. When low-frequency absorption is required, Panel absorbers are often an option. Mounting a thin, flexible panel away from the wall can create a shallow air cavity. The air cavity between the panel and the wall provides a means for sound absorption at particular tuned frequencies. Incident sound at the frequency of interest produces a resonant response in the panel-cavity that causes the panel to vibrate. Filling the cavity with a porous material can reduce the sharpness of the tuning. This type of solution can be cost inhibitive, and can be usually employed to treat a specific tone or narrow band of an offending source, when traditional treatments are insufficient. A traditional approach utilizes a sound absorbing material sandwiched between a perforated lining and an external surface (Figures 5.4 and 5.5). The perforated lining usually consists of sheeting with a pattern of small, evenly spaced holes that can effectively absorb sound at particular tuned frequencies. The perforated facing is mounted on top of the porous material and depending on the thickness, hole size and spacing, can partially act as a panel absorber to increase absorption at certain frequencies (Lam 1995).
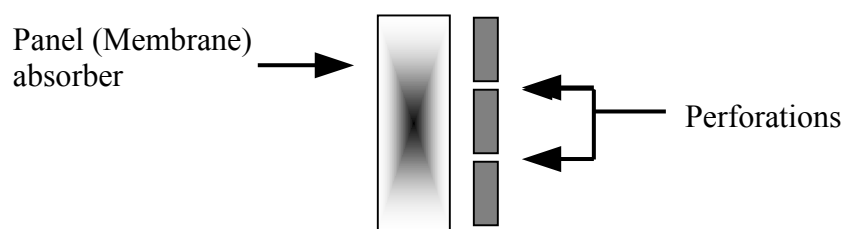
Figure 5.4. Perforated panel absorbers.
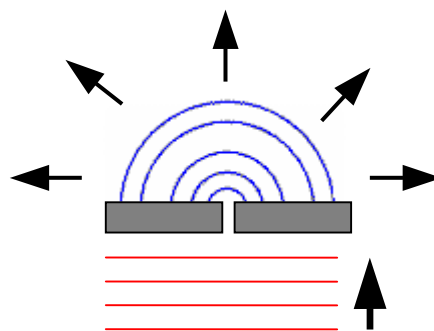
Figure 5.5. Schematic view of waves emerged through a small opening.

5.3. Sound Levels and Intensity

The definition of sound level is not directly given by mathematical equations, but depends on a number of factors such as the intensity of the sound wave, the frequency and the length of the sound exposure, and whether the sound is propagating in air. A measure of sound pressure level is designed to reflect the acuity of the human ear, which does not respond equally to all frequencies. The ear is less efficient at low and high frequencies than at medium or speech-range frequencies. Therefore, to describe a sound containing a wide range of frequencies in a manner representative of the ear's response, it is necessary to reduce the effects of the low and high frequencies with respect to the medium frequencies. The resultant sound level is said to be A-weighted. The A-weighted sound level is also called the noise level. Sound level meters have an A-weighting network for measuring A-weighted sound level (Ziomek 1995).

The decibel values for some environments typically encountered are listed in Table 5.3 (Raju 2003) and will aid in an understanding of magnitude of the noise produced.

Table 5.3. Decibel values of some environments.
(Source: Raju 2003)

Sound Source	Sound Level, dB	Subjective of human being	Sound Source	Sound Level, dB	Subjective of human being
Rockets and missiles, heavy explosives	150-160	Unbearable	Car at 100 km/hr	70-80	Noisy
Diesel, steam engine and ball mills, crackers	120	Unbearable	Office complex, average loudness of voice	60	Noisy
Electric saws and looms, heavy trucks	110	Unbearable	Ordinary room	50	Quiet
Highway vehicles	90-100	Very Noisy	Silent night	30-40	Very quiet

The acoustic intensity, *I*, of a sound wave is defined as the average rate of flow of energy through a unit area normal to the direction of wave propagation. The units for acoustic intensity are joules/sec/m^2, which can also be expressed as watt/m^2. Sound waves radiate outward in a spherical shape. The further a listener is from the sound source, the weaker the loudness of the sound. Intensity and distance can be expressed as:

$$I = L_w / 4 \pi r^2 \tag{5.6}$$

where L_w is the sound power (W), r is the radius or distance from source (m) (Ziomek 1995).

5.4. Sound Absorption Measuring Methods

There are two methods of measuring the sound absorption coefficient of an absorber material. These are the reverberation time method and standing wave tube method (Figures 5.6 and 5.7). Reverberation room method involves placing a unit-area piece of material in a special reverberation room (Figure 5.6) (Urban et al. 2004). The difference in the reverberation time with and without the material yields the absorbing properties of the material. This method is generally more expensive and requiring precisely calibrated sensors and a specially designed reverberation chamber. Although the method does not yield normally incident acoustic impedance data, it is superior for measuring absorption characteristics for randomly incident sound waves and is preferable for determination of absorbing properties that depend on the size of the material. Also, other techniques can measure the sound absorption coefficient in oblique and random incident.
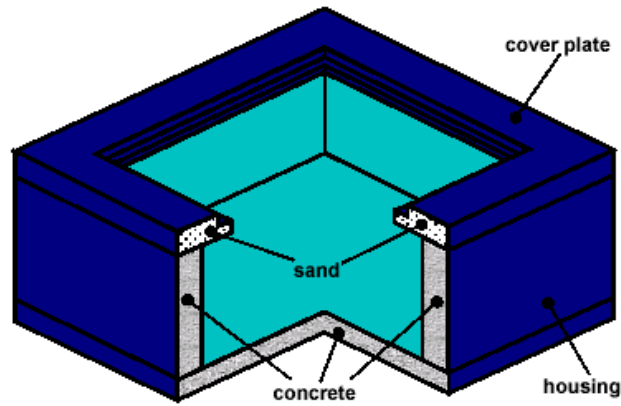
Figure 5.6. Mobile Reverberation room.
(Source: Urban et al. 2004)
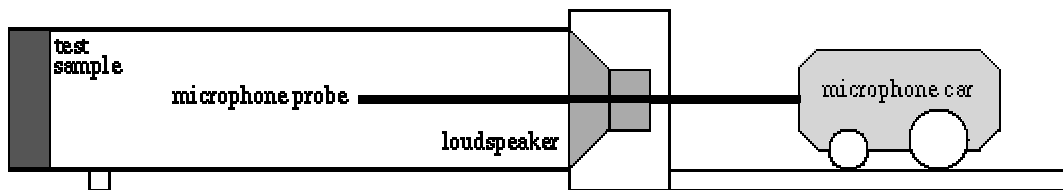
Figure 5.7. Schematic view of standing wave ratio testing device (Impedance tube).
(Source: Biermann et al. 2004)

There are two kinds of standing wave tube method available; transfer method and one-third-octave frequency method. The latter method was used in the present study, which was elaborated in Chapter 6. This method allows one to make quick, easy and perfectly reproducible measurements of absorption coefficient. This measurement makes sound waves to propagate only in one direction in the tube. Therefore, the mathematic problem becomes one-dimensional (in a certain bandwidth). This makes the experimental set-up relatively simple and small. The method also allows for accurate measurement of the normally incident acoustic impedance and requires only small size samples of the absorbing material. In one-third-octave frequency method, each octave band is giving a more detailed description of the frequency content of the noise. Although rarely used for occupational noise measurement, 1/3 octave bands are useful in many environmental, building acoustics and noise control applications.

There are two types of impedance tubes; one has inner diameter of 100 mm and the other one has inner diameter of 30 mm. The measurement frequency is determined by the impedance tube inner diameter (Lu et al. 1999). During the standing wave tube measurements (impedance tube), a loudspeaker produces an acoustic wave, which travels down the pipe and reflects from the testing sample (Figure 5.7) (Biermann et al. 2004). The phase interference between the waves in the pipe, which were incident upon and reflected from the test sample, would result in the formation of a standing wave pattern in the pipe. If 100% of the incident wave was reflected then the incident and reflected waves had the same amplitude; the nodes in the pipe had zero pressure and the antinodes had double the pressure. If some of the incident sound energy was absorbed by the sample then the incident and reflected waves had different amplitudes; the nodes in the pipe no longer had zero pressure.

Figure 5.8 (a) shows the pressure amplitude in the pipe with a rigid end. The entire sound energy incident upon the termination is reflected with the same amplitude. However, there may be some absorption along the walls as the waves travel back and forth along the pipe. Figure 5.8 (b), on the right represents the case when the pipe is terminated with some acoustic absorbing material. Some of the incident sound energy is absorbed by the material so that the reflected waves do not have the same amplitude as incident waves.
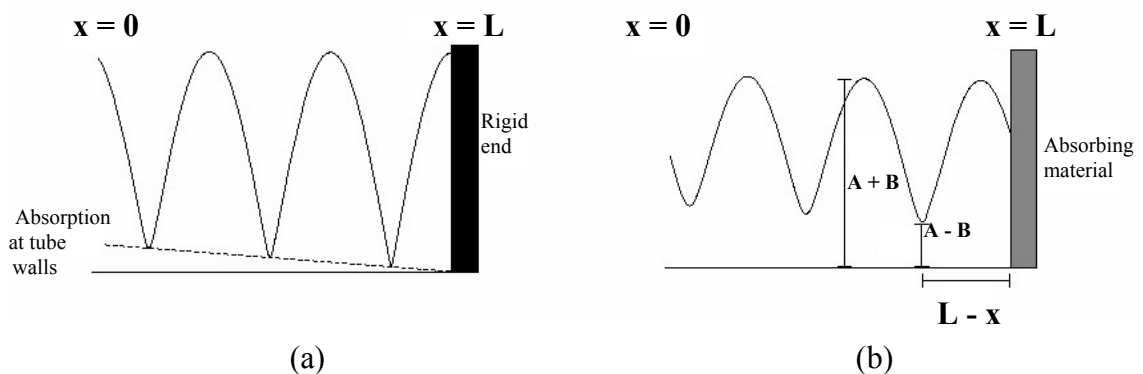
Figure 5.8. (a) Pressure amplitude in the pipe with a rigid end, (b) Pressure amplitude in the pipe with a sound absorbing material.

In standing wave ratio technique, the pressure amplitudes at antinodes (maximum pressure) and nodes (minimum pressure) are measured with a microphone

probe attached to a car that slides along a graduated ruler. By means of the movable microphone, the ratio of the pressure maximum to the pressure minimum is determined. The ratio of the pressure maximum (antinode) to the pressure minimum (node) is called the standing wave ratio (*SWR)*. It can be calculated with the following equation:

$$SWR = \frac{A+B}{A-B}$$ (5.7)

During the sound absorption coefficient measurements, the microphone car is slightly moved until the maximum level (*A+B*) is indicated by the cursor reading, for a specific frequency, and it is recorded, after this, the microphone car is moved until the minimum level (*A-B*) was indicated by the cursor reading, for specific frequency and it is recorded. It is not possible to measure *A* or *B* directly so that these values are measured by the standing wave tube. By means of the ruled scale under the movable microphone, the position of the first minimum pressure (*A-B*) from the foam sample to the end of the tube (ΔL) is recorded and it can be expressed by the following equation:

$$\Delta L = 20 \ log \ SWR = (L\text{-}x)$$ (5.8)

then *SWR* can be also expressed as follows;

$$SWR = 10^{\frac{\Delta L}{20}}$$ (5.9)

This *SWR* value is used to determine the sample's reflection coefficient amplitude *R*, its absorption coefficient α and its impedance *Z*. Equation 5.7 can be arranged in order to provide the sound power reflection coefficient:

$$R = \frac{SWR-1}{SWR+1}$$ (5.10)

Sound absorption coefficient for the test sample at a given frequency is given by the below equation:

$$\alpha = 1 - R^2 = 1 - \frac{(SWR-1)^2}{(SWR+1)^2} \tag{5.11}$$

By using the Equation 5.9 (Woodack 2000), it can be also expressed by the following formula:

$$\alpha = \frac{4.10^{\frac{\Delta L}{20}}}{(10^{\frac{\Delta L}{20}} + 1)^2} \tag{5.12}$$

5.5. Sound Absorption in Metal Foams

Lu et al. (1999) conducted several experimental studies on the sound absorption capacity of Alporas closed cell aluminum foams. Their experimental results showed that thus hole drilling, rolling and compression increased the sound absorption in these foams. Also they investigated the viscous and thermal effects in sound absorption and they concluded that sound absorbed by viscous flow across small cracks appeared to dominate the overall sound absorption capacity. Their experimental results showed that viscous effect was comparable to thermal effect when the foam was relatively thin ($L \cong$ 1 cm), but became dominant at high frequencies ($f >$ 1000 Hz) when the foam was relatively thick ($L \cong$ 10 cm) also increasing the pore size increased sound absorption. They concluded that sound absorption due to viscous and thermal losses alone was not significant unless the cell size is on the order of submillimeters. Han et al. (2003) investigated the acoustic absorption behavior of open cell aluminum foam. Their results showed that for maximum absorption coefficient, noise reduction coefficient (NRC) and half-width of the absorption peak were 0.96-0.99, 0.44-0.62 and 1500-3500 Hz, respectively. They concluded that sound absorption mechanism in the open cell foams was occurred by viscous and thermal losses when there was no air-gap backing and it was occurred by Helmholtz resonance effect when there was an air-gap backing behind the foam sample. They observed that Al foams with small pore sizes have smaller absorption coefficients. Moreover, their experimental results showed that NRC was decreased with increasing pore size when there was no air gap behind foam sample. Biermann et al. (2004) investigated the reduction of tire, door and interior car noise and

truck noise by use of metallic foams and sandwich foam panels, while Urban et al. (2004) investigated body acoustics and power train noise reduction by using semi-opened metallic foams. Huebelt et al. found that the acoustic performance of hollow spheres depended upon the sphere diameter and sintering temperature. Park et al. (2004) conducted measurements on the acoustic properties of porous and granular materials. They measured the transfer function between the excitation and the response, under controlled longitudinal vibration. The wave propagation characteristics, wave speeds and their loss factors were determined from the measured transfer function. They analyzed their measurement results' characteristics using the linear visco-elastic theory. They investigated the impact of several parameters such as vibration amplitudes, static loading, and particle size, on the measured dynamic properties. Xu et al. (2004) developed a two-dimensional, closed-form analytical approach to predict the acoustic attenuation of a perforated single-pass, concentric cylindrical expansion chamber filled with fibrous material. They used the boundary conditions at the central, perforated screen, and rigid wall. They obtained the governing eigenequation, which determined the sound field in the dissipative chamber. They predicted the transmission loss by the eigenvalues and eigenfunctions, by applying the pressure and particle velocity matching at the interfaces of the expansion and contraction. Their analytical predictions showed well agreements with their experimental results within the frequency range of interest.

CHAPTER 6

MATERIALS AND TESTING

6.1. Al and SiC/Al Foam Preparation

Aluminum closed cell foams were prepared using the foaming from powder compacts (precursors) process, patented by Fraunhofer CMAM (Baumeister and Schrader 1992). The process started with the mixing of appropriate amounts of basic ingredients, Al powder, SiC_p (10 wt.%) and TiH_2 (1 wt.%), inside a plastic container, which was rotated on a rotary mill in order to form a homogeneous powder mixture (Figure 6.1) (Kavi 2004). The average particle size of the Al and SiC_p were 34.64 and 22.36 μm, respectively and the size of TiH_2 particles was less than 37 μm. The specification of raw materials used is given elsewhere (Elbir 2001). In the second stage of the process, the powder mixture was initially cold compacted inside a rectangular ST 37 steel die, having a cross-section of 70 x 70 mm (Figure 6.2 (a)), under a pressure of 200 MPa. The compacts having 80% relative density were then open-die hot-forged at a temperature of 350 ^{o}C, resulting in foamable precursor materials with the final densities of 98% and thicknesses of approximately 8 mm (Figure 6.2 (b)). As a result of open die forging, the cross-sectional area of the precursor increased and small cracks were formed at the edges of the precursor. In order to remove the cracks, the cross-sectional area of hot-forged precursor was machined into the dimensions of 70 x 70 mm, same with the cross-sectional dimensions of the foaming molds (Figure 6.2 (c)). The flat side surfaces of the precursor also provided good thermal contact with the foaming mold. Foaming experiments were conducted in a pre-heated furnace at a temperature of 750 ^{o}C. The precursor was inserted into a pre-heated steel mold providing expansion only in the vertical direction (Figure 6.3). After precursor insertion, the steel mold (closed at the bottom) was closed at the top (Figure 6.3). The inserting and removing specimen took less than 10 seconds. The liquid foam was finally water-quenched. Using above methods plates of Al and SiC/foam samples having cross-sections of 7 x 7 x 4 cm (Figure 6.4) were prepared for thermal and sound absorption tests. Totally 8 Al and composite and 4 Al and 5 composite foam samples were prepared for effective thermal and sound measurements, respectively.

Al powder   **TiH$_2$**

Mixing of the powders

Pressing of the blend

Thinning of the precursor

Processing of the precursor
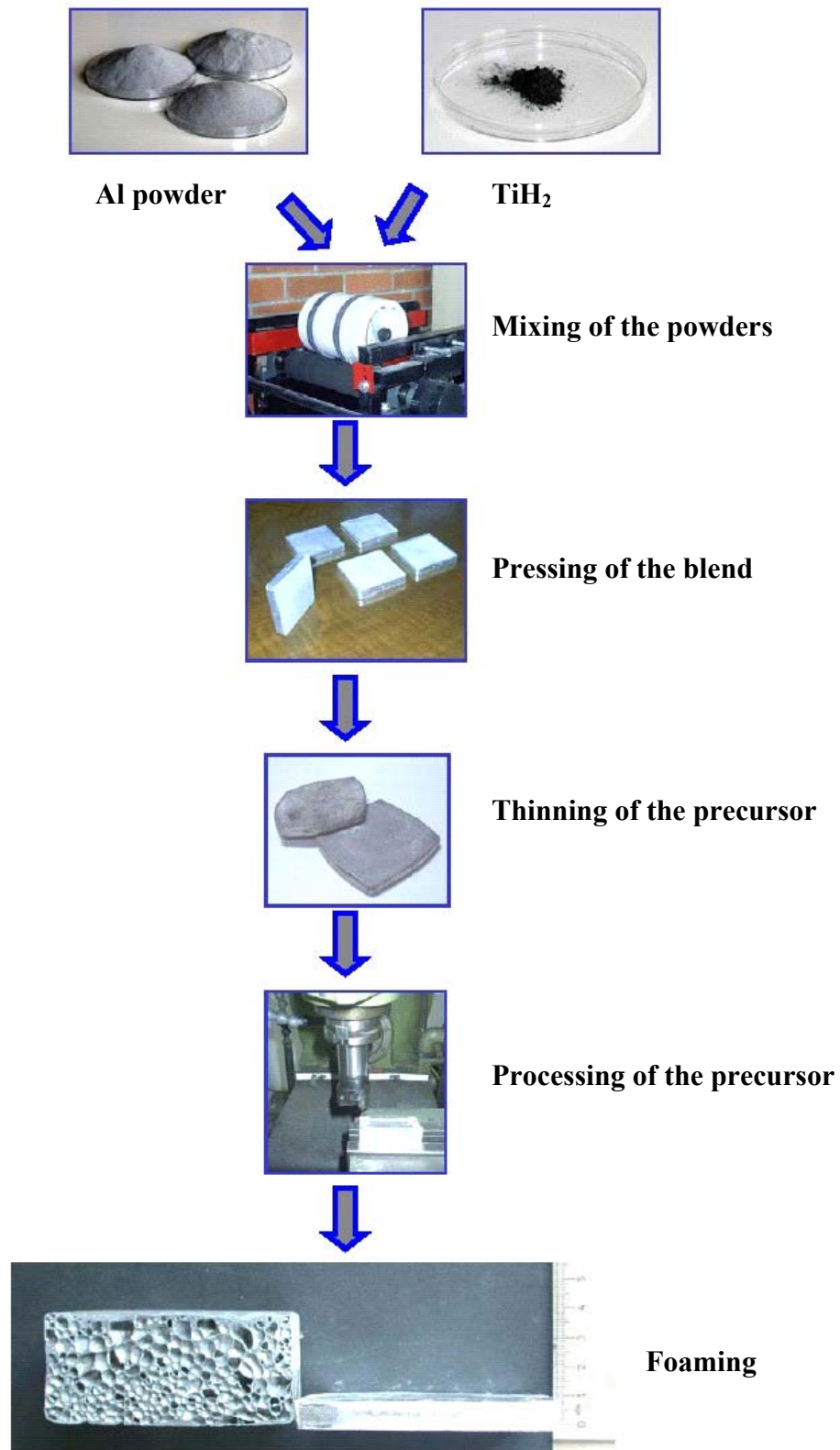
Foaming

Figure 6.1. Schematic of foam preparation process
(Source: Kavi 2004).
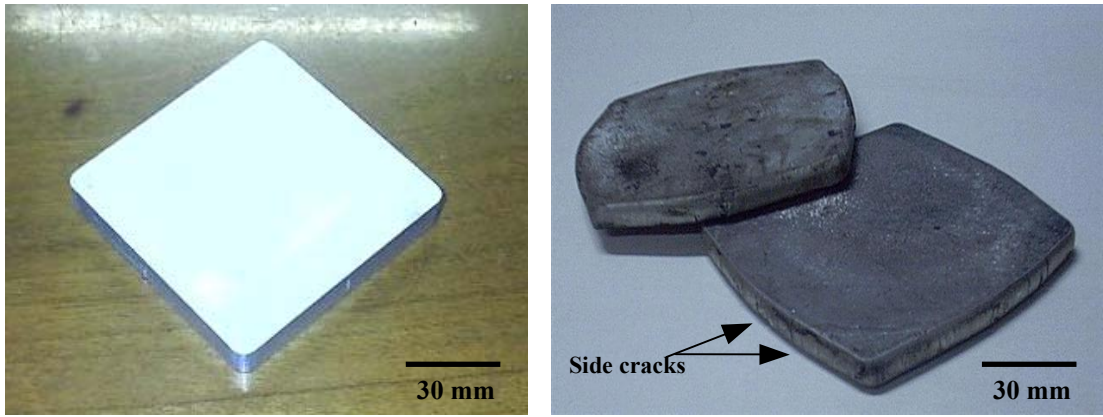
(a)

(b)
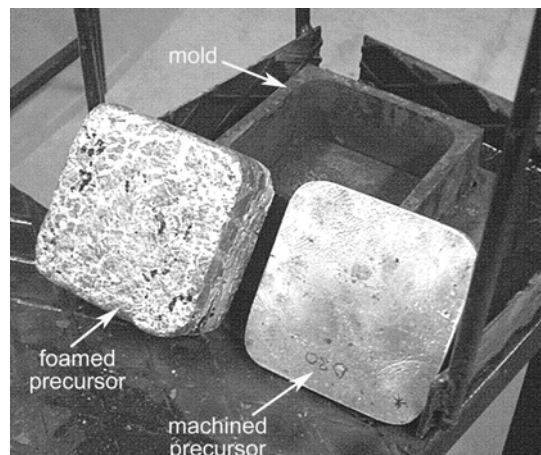
(c)

Figure 6.2. (a) Cold compacted precursor, (b) precursor after hot-forging and (c) machined and foamed precursor.
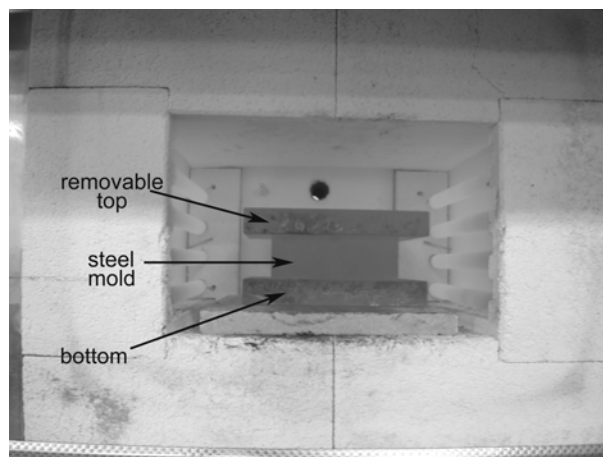
Figure 6.3. Foaming in the furnace with a steel mold closed at the top and bottom.

Figure 6.4. Al foam sample after cooling process.

6.2. Foam Sample Machining

Samples for effective thermal conductivity (ETC) and sound absorption measurements were core drilled using electro-discharge machine normal to the foaming direction of the prepared Al and SiC/Al plates (Figure 6.5). Since the foam plates contained a dense metal layer at/near the surface and relatively homogeneous density in the mid sections, core drilling was performed through the midsection. Initially 70 mm long samples were machined, then these samples were sliced into smaller pieces using diamond saw. The samples used in the effective thermal conductivity and sound absorption measurements were 25 mm in diameter and 30 mm in height and 30 mm in diameter and 10 mm in height (Figures 6.6 and 6.7). Totally, 29 Al foam and 30 SiC/Al foam samples with varying densities were measured for ETC while 11 Al foam and 16 SiC/Al foam samples were used in sound absorption tests. The use of electro-discharge machine minimized damage to the cells and resulted in relatively smooth sample surfaces. The sliced surfaces of the samples were grinded and polished before the measurements. After machining, the samples were washed with alcohol and then dried for 2 hours at 180 $^{\circ}$C in an oven. Densities of the foams were measured by the ratio of weight to the volume of the samples. The properties of samples used in ETC and sound absorption tests are listed in Appendix A and B, respectively.
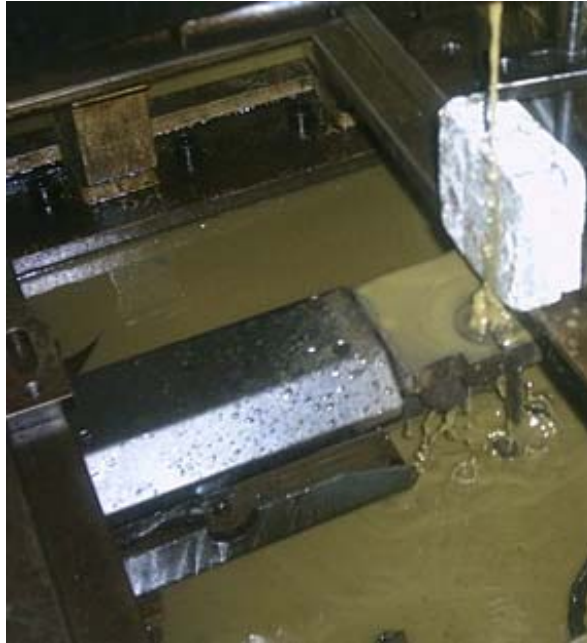
Figure 6.5. Electro-discharge cutting normal to foaming direction.

Figure 6.6. Cylindrical foam sample for effective thermal conductivity test.

Figure 6.7. Cylindrical foam sample for sound absorption test.

6.3. Effective Thermal Conductivity Measurements

Effective thermal conductivity (ETC) was measured using temperature distribution for steady state conduction through a uniform plane wall method. The set-up used is shown in Figures 6.8 (a) and (b). Thermal tests were conducted using a Heat transfer testing unit H110 (Figure 6.9 (a)). The transfer module was cylindrical and mounted with its axis vertical on a base plate. The heated section of the set-up houses a 25 mm diameter cylindrical brass section with a nominally 60 watt (at 24V DC) cartridge heater in the top end. Three fixed thermocouples T_1, T_2, T_3 were positioned along the heated section at 15 mm intervals. The transfer module was water-cooled at its bottom end by water flowing through galleries. Thermocouples T_6, T_7, T_8 were placed along this section at 15 mm intervals. In atypical experiment a foam sample was placed in between the heating and cooling sections and a constant voltage (10.0 V) and current (1.04 A) were applied. The sample was insulated by a polystyrene foam with a low thermal conductivity of 0.10-0.16 (Figure 6.9 (b)) such that the thermal conductivity of

the surrounding foam is negligible (Lienhard IV and Lienhard V 2001). The thermal conductivity measurement was made when the readings of the thermocouples T_1, T_2, T_3, T_6, T_7 and T_8 reach to constant values, also called steady-state condition. It was found that steady state condition was reached when the temperature reached at 123 $^{\circ}$C - 123.5 $^{\circ}$C for both Al and SiC/Al foams.
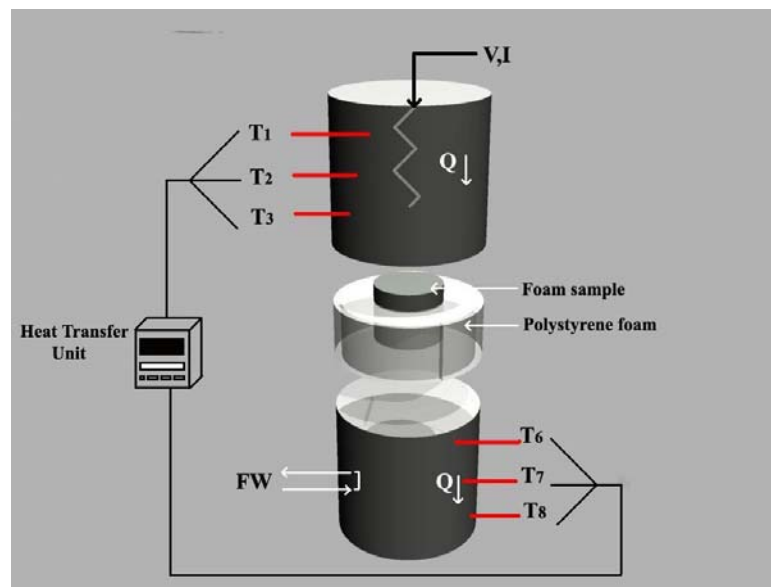
(a)
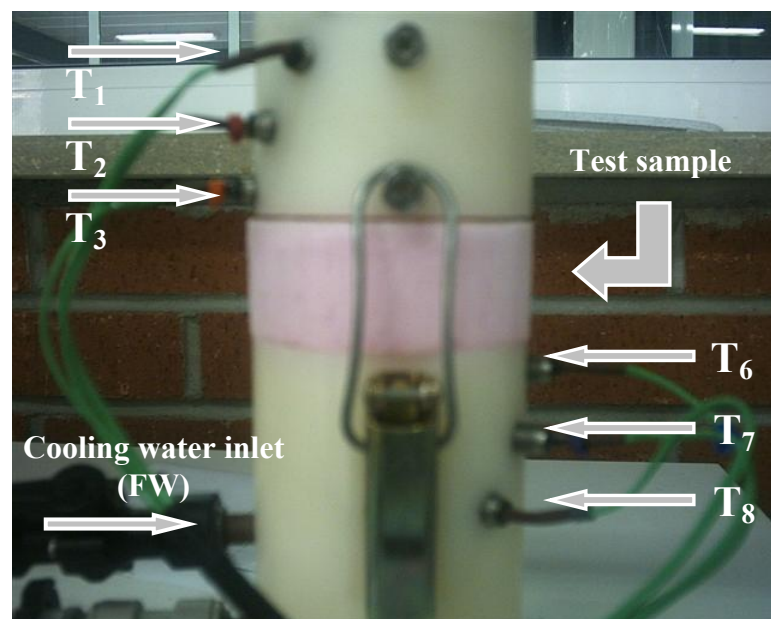
(b)

Figure 6.8. Thermal conductivity measurement set-up (a) schematic and (b) side view.
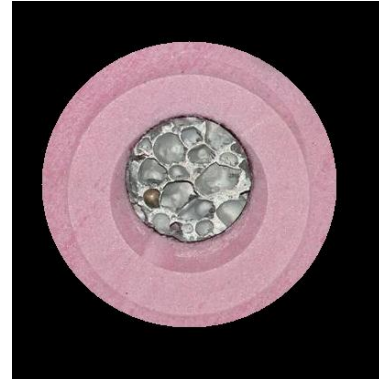
Figure 6.9. (a) Thermal conductivity heating unit and (b) Al foam test sample covered by polystyrene foam.

The heat transfer rate (Q) by conduction through a plane wall, which has a thickness of (Δx) and an area of (A) is can be calculated by Equation 4.2. Q can also be expressed with the following equation:

$$Q = V \cdot I \quad (W) \tag{6.1}$$

Assuming the temperature distribution along heat transfer unit is linear, the temperatures of hot face ($T_{hotface}$) and cold face are calculated using following relations,

$$T_{hotface} = \frac{T_3 - (T_2 - T_3)}{2} \tag{6.2}$$

$$T_{coldface} = \frac{T_6 + (T_6 - T_7)}{2} \tag{6.3}$$

Under steady state conditions, the heat transfer rate equation is,

$$Q = -\frac{kA(T_{coldface} - T_{hotface})}{\Delta x} \tag{6.4}$$

Therefore, using Equations 6.1, 6.2, 6.3 and 6.4, one can easily calculate the effective thermal conductivity.

6.4. Sound Absorption Measurements

Sound absorption was measured using standing wave ratio method, using a computer controlled Brüel & Kjær Standing Wave Apparatus Type 4002, along with the B&K Real-Time Frequency Analyzer Type 2133 (1/3 Octave Band Analyzer) testing machine at Tofaş. For each samples at least two tests applied and the results were found varying insignificantly and averaged. The test set-up used is shown in Figure 6.10 schematically and had a standing wave tube with an internal diameter of 30 mm and a length of 1 m. The device is conventionally used for sound absorption measurements in the low-frequency ranges, from 80 Hz to 2000 Hz (Woodack 2000).
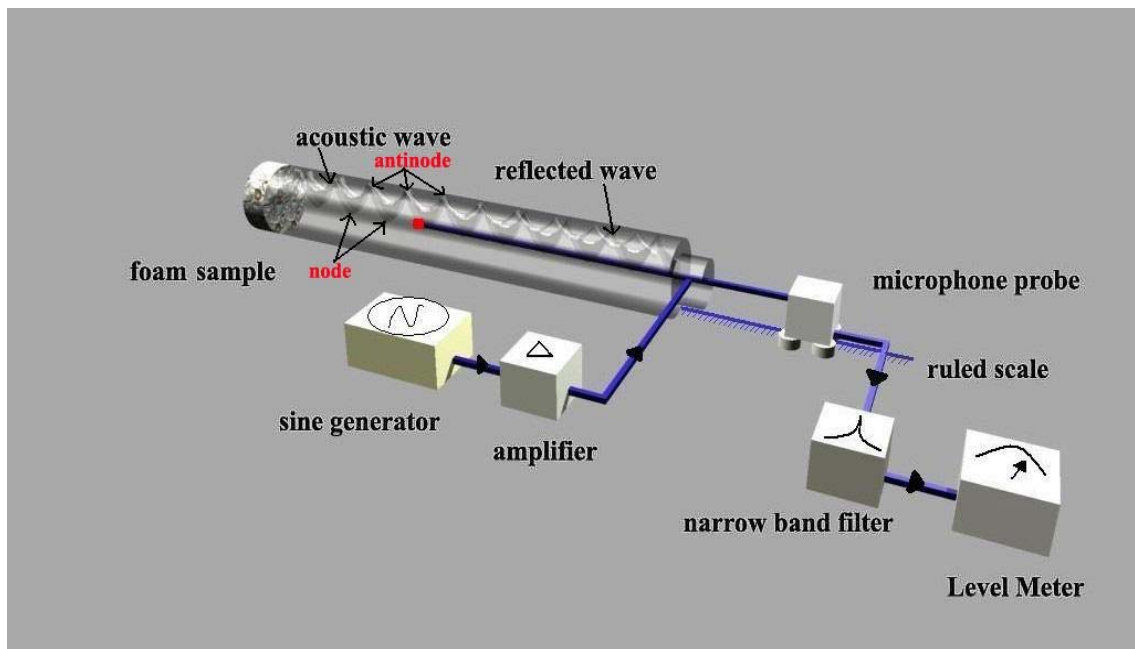
Figure 6.10. Schematic view of standing wave ratio test set-up used for the sound measurements.

Before measurements conducted, four initial tests were performed to determine the sound absorption test parameters in order to minimize errors in the actual measurements. During these tests, the sound absorption coefficient of the back plate located at the end of the standing wave ratio tube was measured 0.025 on average at 200-1600 Hz. Hence, the sound absorption coefficient of the rigid wall was neglected. However, during the tests, relatively small amount of sound energy dissipates due to

viscous and thermal effects of the tube walls and attenuation along the air path. Therefore, the cavities around the sample were covered by vaseline to create a complete incidence surface.

In a typical test, a foam test sample was placed into the impedance tube and the cap was clamped tightly (Figure 6.10). The bandwidth was set to 1/3 octave from 200 Hz to 1700 Hz. The loudspeaker arranged to produce an acoustic wave, which traveled down the pipe and reflected from the foam samples. Standing wave pattern in the tube was formed by the phase differences between the incident and reflected waves. Nine 1/3 octave bands, which were clearly observed on the level meter were selected for measuring the sound absorptions of the foam samples (250, 315, 400, 500, 630, 800, 1000, 1250, 1600 Hz). Initially, the generator was set to the 250 Hz sine wave. The maximum and minimum levels were recorded that was indicated by the cursor reading on the level meter by moving the microphone probe, for 250 Hz. By using the ruled scale under the microphone probe, the position of the first minimum pressure (node) from the foam sample to the end of the tube was recorded (Figure 6.11), by inserting this ΔL value (L-x) to Equation 5.12, sound absorption coefficient α was found for each sample. This process was done for the other frequency (1/3 octave) bands.
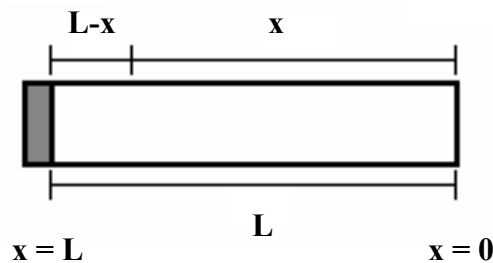
Figure 6.11. Position of the first minimum pressure (node) ΔL from the foam sample.

Samples with holes were also tested for sound absorption properties. Initially 1.5 mm-hole-drilled samples were tested and then on the same samples the hole size increased to 2.5 mm. (Figure 6.12). The same sound absorption measurement procedure was applied to the drilled samples as outlined in the Section 6.3.
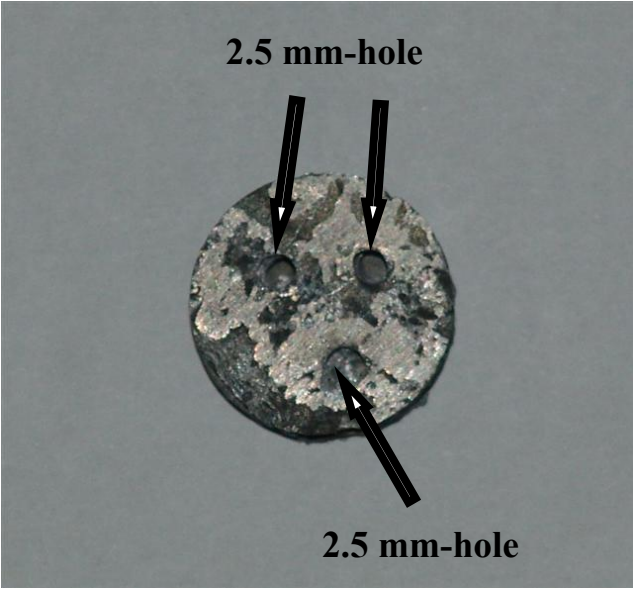
Figure 6.12. 2.5 mm-hole-drilled foam sample.

CHAPTER 7

RESULTS AND DISCUSSION

7.1. Foaming Experiments

Relatively high densities of the precursors are needed for an efficient foaming. It was observed that the cold compaction process applied at 200 MPa yielded a relative density of 80%. Initial foaming experiments on cold compacted precursor resulted in partial foaming, two or three times increase in the thickness of the precursor. The hot compaction process (300 ^{o}C) applied to the cold compacted precursor at 400 MPa increased the relative density above 98% for both Al and SiC/Al precursors. The previous foaming studies on the same Al and SiC/Al compacts in a box furnace at 750°C showed that linear expansion could reach as high as 4-5 (Elbir 2001). The furnace and precursor temperature-time history of a precursor in the furnace, shown in Figure 7.1, represents the important stages of foaming process. Since the precursor material was inserted into the preheated foaming mold at room temperature, the foaming started only after a time. Initially the precursor temperature increased to 700 ^{o}C (over heating) and this was followed by the melting of the precursor at 663 ^{o}C as depicted in Figure 7.1. It is also seen in the same figure, the foaming started only after 5 min 20 seconds and precursor material filled the foaming mould completely at 6 min 25 seconds. Figures 7.2 (a) through (d) show the foamed precursor material taken from the furnace at various furnace holding times and then quenched.

Foaming mold, its material, the type and size of the furnace are all effective in the foaming process. In this study, ST 37 steel foaming molds were used for both Al and SiC/Al foaming. The linear expansion of the foam precursor for any prescribed furnace holding time was found to be quite repeatable as long as the foaming and heating conditions were carefully adjusted and controlled, e.g. preheating temperature and the time for inserting into and removing the precursor from the mold. It should also be noted that the precursor material was indirectly heated through the heat conduction from the preheated foaming mold (50 min.) to the precursor. When the expansion of precursor reaches to a prescribed height, the liquid foam should be taken from the furnace and solidified quickly in order to retain its shape and cell structure in the solid

state. Otherwise, the molten aluminum flows downwards at longer foaming durations, a natural process known as drainage, and forms a dense metal layer at the bottom of the precursor. The longer furnace holding times also resulted in the collapse of cell walls leading to non-uniform and very large cell sizes (Elbir 2001). The solidification of the liquid foam is also quite complex and difficult to describe. In the cooling stage, geometrical defects (Figures 7.3 (a) and (b)) mostly arising from the inhomogeneous cooling rates were observed. The foamed precursors that contained defects were discarded.
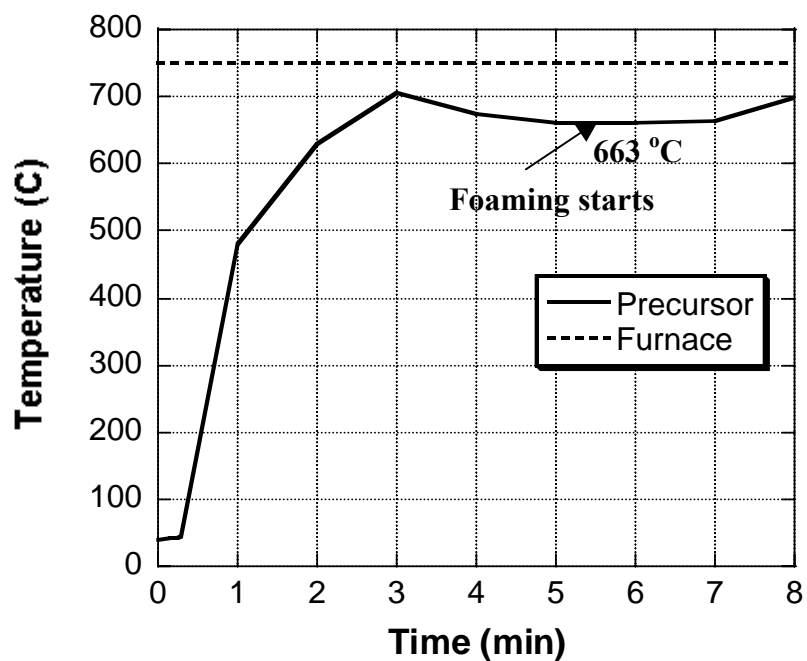
Figure 7.1. Variation of furnace and precursor temperature *vs.* time.

Figure 7.2. Foamed precursors taken from the furnace at various furnace holding times (a) 6 minutes 25 seconds (b) 6 minutes 15 seconds (c) 5 minutes 40 seconds (d) 5 minutes 20 seconds.

Figure 7.3. Typical geometrical defects found in the foamed precursor: collapse at the (a) bottom and (b) top of the foamed plate.

In the foaming of powder compact process, foam stabilization was ascribed to the metal oxide filaments, which are remnants of the thin oxide layer on the aluminum powders and/or the solid component of the particular alloy. The presence of solid particles plays a critical role in liquid foam stabilization through increasing melt bulk viscosity and contributing to increasing surface viscosity of the cell faces if a significant fraction of particles is located at the gas/melt interface. Both are effective in slowing down capillarity-driven melt flow from cell faces through cell edges (cell thinning) and gravity driven melt flow through cell edges (drainage).

7.2. Effective Thermal Conductivity of Al and SiC/Al Foams

The variation of the ETCs of Al and SiC/Al foams with porosity and relative density are shown sequentially in Figures 7.4 (a) and (b). The ETCs of foams increase with increasing relative density (Figure 7.4 (a)) and decrease with increasing porosity (Figure 7.4 (b)). At a porosity of 86% the ETC of Al foam decreases from 9 W/m K to about 5 W/m K, when the porosity increases from 86% to 92%, while, the ETC of SiC/Al foams decreases from 7.5 to 5 W/m K within the same porosity range (Figure 7.4(b)). As seen in the same figures, SiC/Al foam samples show lower values of ETCs than Al foams within the studied relative density range. It is also seen in Figures 7.4 (a) and (b) the difference between the ETCs of SiC/Al and Al foams decreases with decreasing relative density and/or increasing porosity. At 92% porosity the ETCs of the foams become very similar to each other (Figure 7.4 (b)). The ETC measurements of Al and SiC/Al foam samples are listed in Appendix A.

The results of this study show that SiC particles can be used to tailor the ETCs of Al foams for functional applications. As the porosity increases above 90% the effect of SiC particles on the reduction of effective thermal conductivity vanishes for the reason of the dominating effect of low thermal conductivity of the air contained within the cells. When structural applications are considered the fraction of SiC particles should be chosen carefully since SiC particles may decrease the ductility of the foam greatly at relatively high concentrations (Guden and Yuksel 2005).
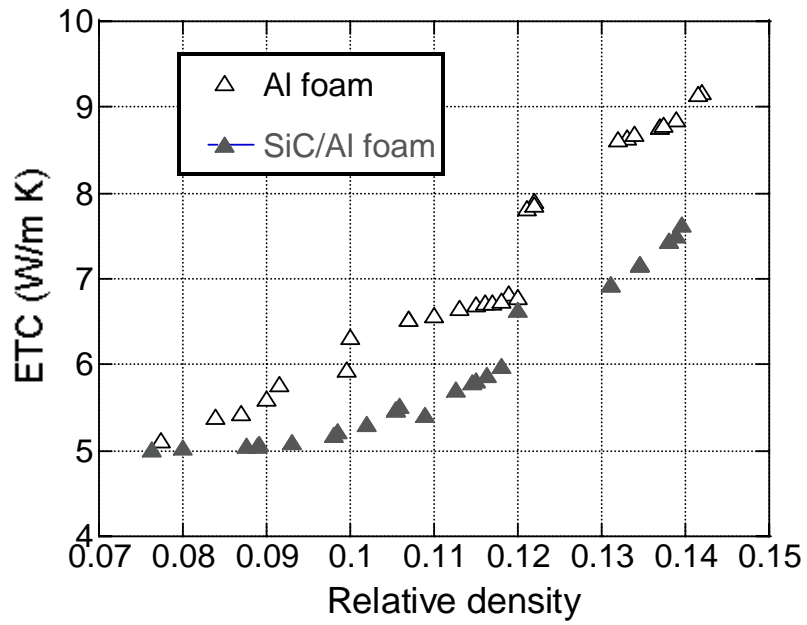
(a)
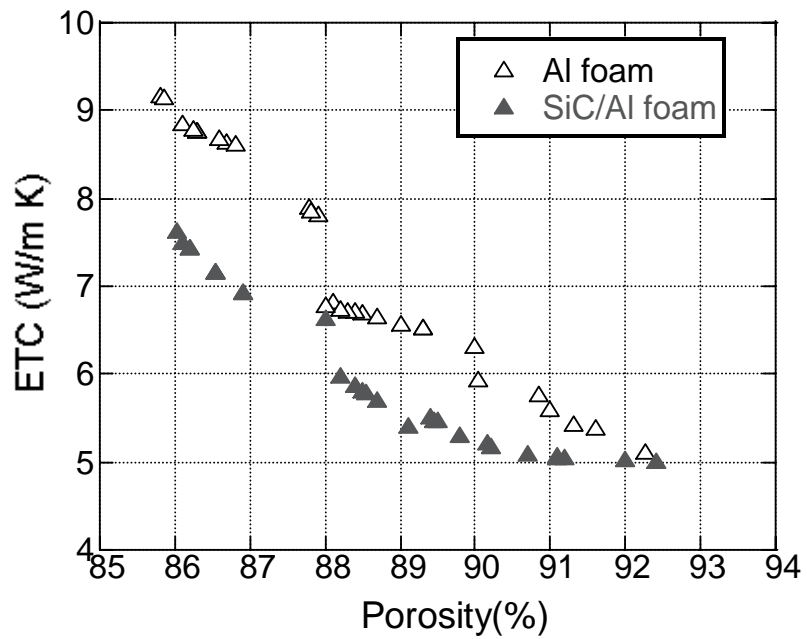
(b)

Figure 7.4. Effective thermal conductivities of Al and SiC/Al foams as function of
(a) relative density and (b) porosity.

7.3. Models of Thermal Conduction and Comparison with Previous Studies

The results of ETC measurements were fitted to the previously used ETC models of open and closed-cell foams given in Chapter 4. In the fitting process following approximate ETC values at 125 $^{\circ}$C were used: k_{Al}=206 W/m·K (Horn 1967), $k_{g(air)}$ = 0.026 W/m·K (Lienhard IV and Lienhard V 2001) and k_{SiC}= 100 W/m·K (Clyne and Withers 1993). The thermal conductivity of the composite matrix ($k_{composite}$) in SiC/Al foam was calculated using the rule of mixtures as

$$k_{comp} = fk_{SiC} + (1-f)k_{Al} \tag{7.1}$$

where f is the volume fraction of the SiC particles and k_{comp} is the thermal conductivity of the composite material. Figures 7.5 (a) and (b) show sequentially the fitting of the ETC values of Al and SiC/Al foams to Equations 4.10 and 4.11. Both equations predict very similar ETC values and therefore can not be differentiated on the same graph. The *A* values in Equation 4.10 were calculated as 0.30 and 0.27 for Al and SiC/Al foams, respectively. The values of *A* given in Equation 4.11 were 0.091 and 0.075 for Al and SiC/Al foams, respectively. Despite to small variation, the fitting of experimental ETC values of Al and SiC/foams gave similar *A* values. It also noted in Figures 7.5 (a) and (b) that Equations 4.10 and 4.11 can not predict the ETC values above 90% porosity satisfactorily.

The fitting of the ETC values of Al and SiC/Al foams to Equations 4.12 and 4.17 (Bhattacharya et al. (2002) and Boomsma and Poulikakos (2001) models) resulted in very high deviations from the ETC values of Al foams (16.7% and 42.6%). Therefore, these models could not be used to predict the ETC values of present Al and SiC/Al foams.
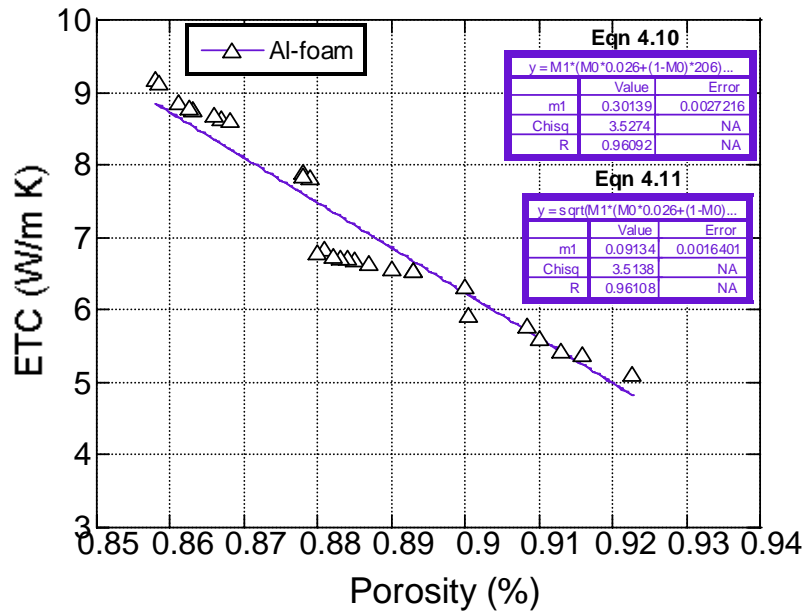
(a)
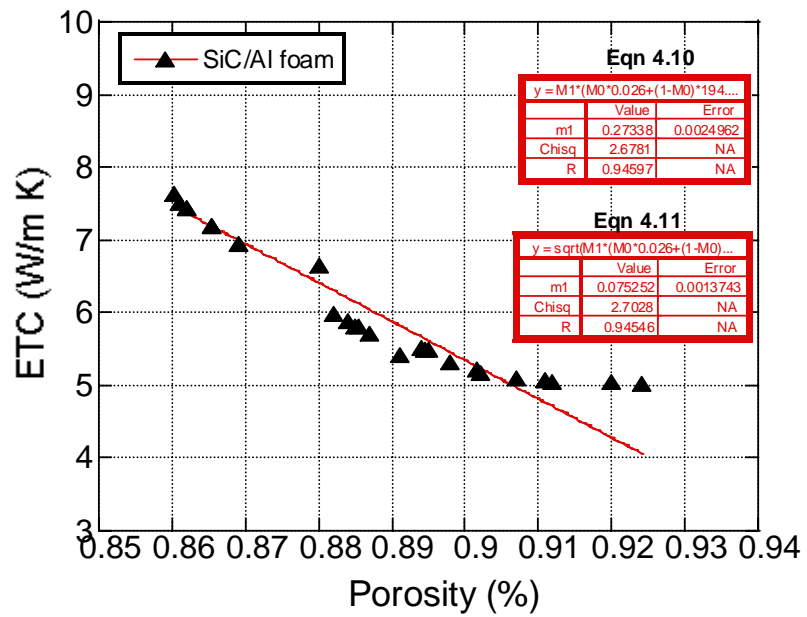
(b)

Figure 7.5. Fitting of experimental ETC values to Equation 4.10 and 4.11,
(a) Al and (b) SiC/Al foams.

The values of A in Equation 4.13 and 4.16 were determined by fitting the experimental ETC values of Al and SiC/Al foams to Equation 4.13. The results of fitting are shown in Figure 7.6 for Al and SiC/Al foams. The values of A for both foams are almost not changing with porosity within the studied porosity range. The average values of A in Figure 7.6 are 0.82 for Al and 0.80 for SiC/Al foams. These results are contrary to the results of Singh and Kasana (2004) who found that the value of A increased with logarithm of porosity for the ERG open cell foams. A second degree polynomial fit to the values of A in Figure 7.6 also gives higher regression constants for both foams as shown in the same figure. As shown in Figures 7.7 (a) and (b), when the value of A shows a second degree of polynomial dependence on the porosity the experimental and predicted values of ETCs show well agreement.

The fitting of the ETC values of Al and SiC/Al foams to Equation 4.24 is shown in Figure 7.8. The regression constants of fitting for both foams are comparable with Equations 4.10 and 4.13 (when A is constant).

Based on above results, the best fit is found with Equation 4.13 using polynomial fit to the value of A. Therefore the following Equations are proposed to predict the ETCs of the present Al and SiC/Al foams within the porosity range of 85-92%;

$$k_e = k_{parallel}{}^{A} . k_{series}{}^{(1-A)} \qquad (7.2)$$

$$A = 11.449 - 23.692\,\phi + 13.194\,\phi^2 \quad \text{for Al foam} \qquad (7.3)$$

$$A = 17.943 - 38.596\,\phi + 21.722\,\phi^2 \quad \text{for SiC/Al foam} \qquad (7.4)$$
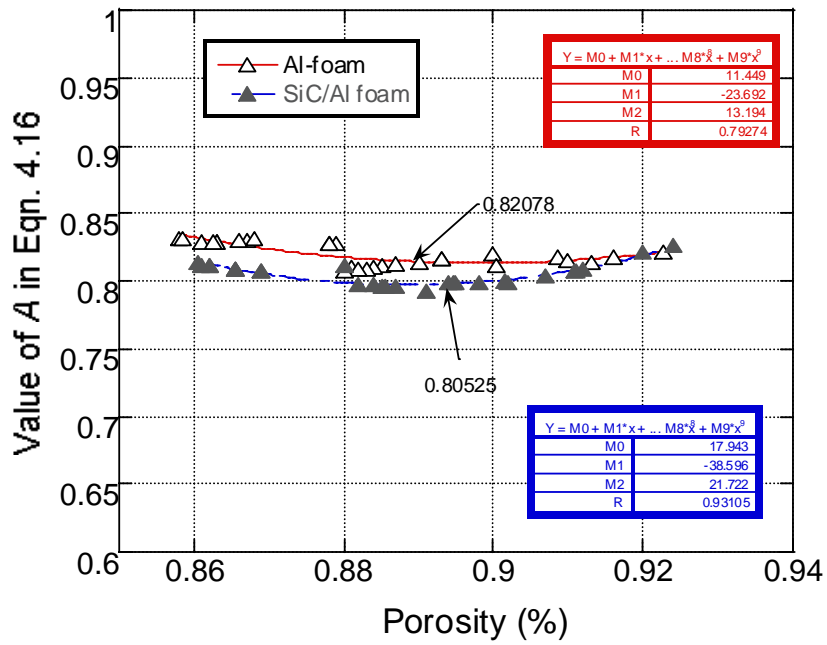
Figure 7.6. Fitting of *A* values of Equation 4.13 using Equation 4.16 to the experimental values.
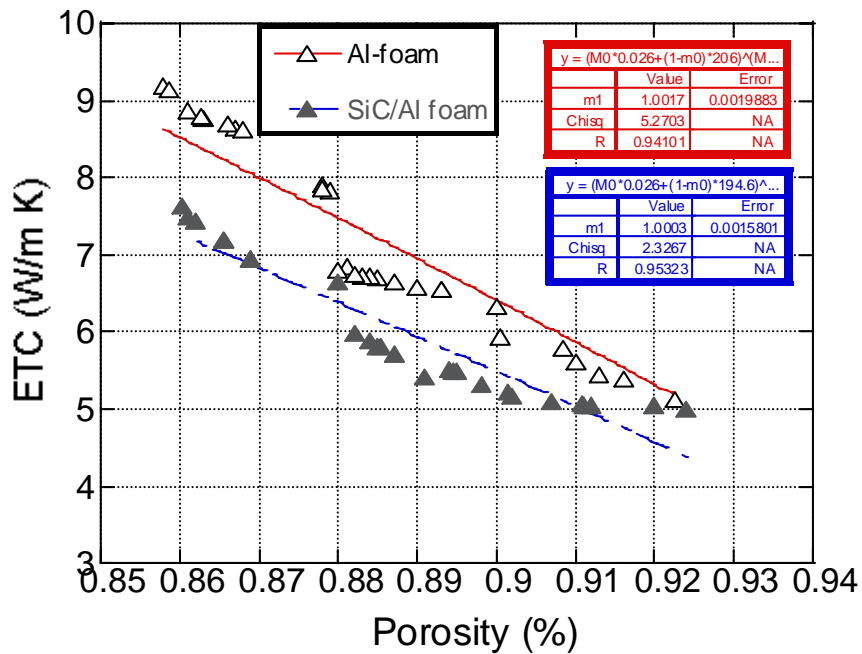
(a)
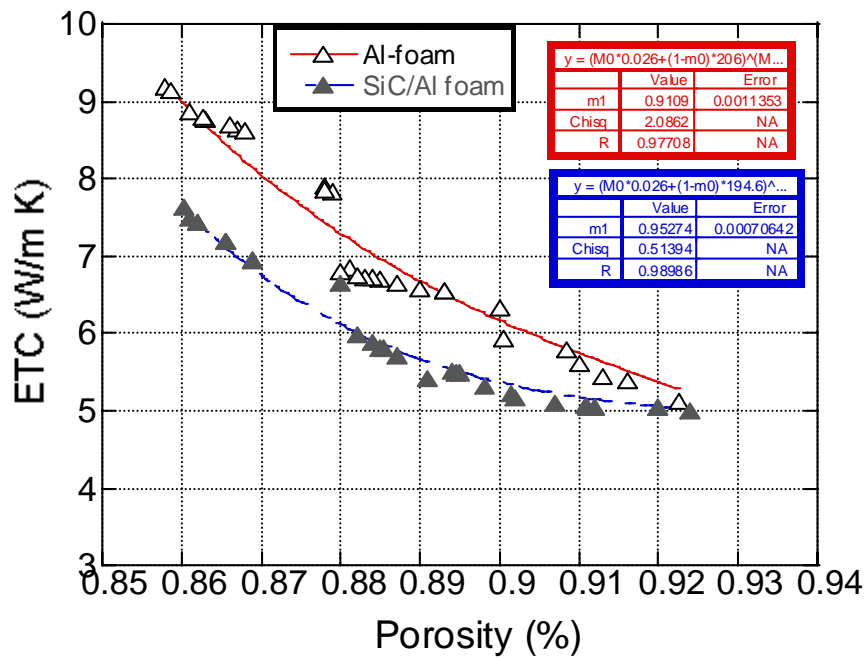
(b)

Figure 7.7. Fitting of experimental ETC values to Equation 4.13, when (a) *A* is constant and (b) *A* shows a second degree of polynomial dependence on the porosity.
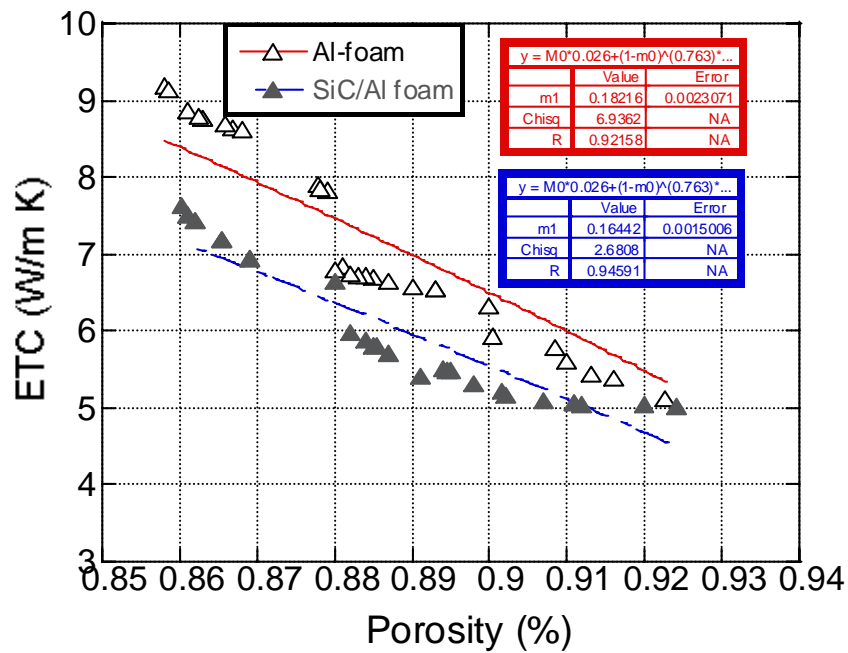
Figure 7.8. Fitting of experimental ETC values to Equation 4.24.

In Figure 7.9 the ETCs of present Al and Alporas closed foams and ERG open cell foams are shown as function porosity. The present Al foams show lower ETC values as compared with Alporas and ERG foams. Alporas and ERG foams are produced by melting process while present foams are processed through powder metallurgical route. In the foaming powder compact process the metal oxide filaments, which are remnants of the thin oxide, layer on the aluminum powders and/or the solid component of the particular alloy remains in the cell walls and edges. These oxide particles may greatly reduce the thermal conductivity of the foam as compared with liquid foam processing methods. Microscopic analysis of the cell walls also confirms this fact: the boundaries between the original particles are clearly seen in Figure 7.10.
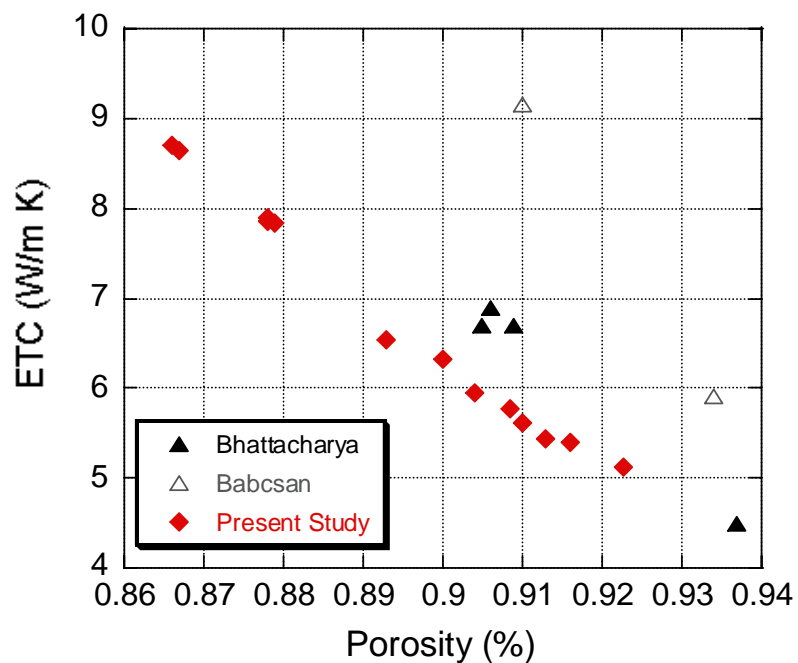
Figure 7.9. Comparison of ETCs of Al foams with Alporas and ERG foams.
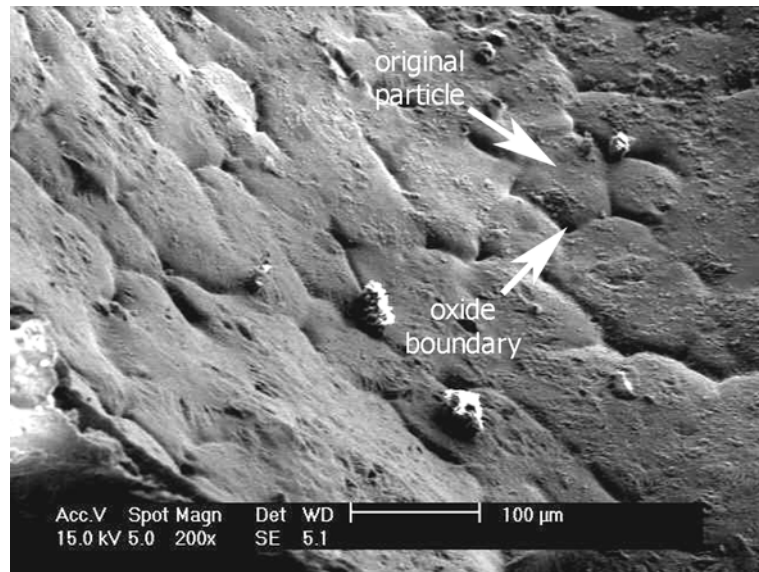
Figure 7.10. Scanning electron microscope image of cell wall surfaces showing original particle boundaries.

7.4. Sound Absorption Behavior of Al and SiC/Al Foams

Figures 7.11 (a) and (b) show the variations of the sound absorption coefficients of Al and SiC/Al foams at two different relative densities between two tests conducted on the same sample within the studied frequencies, respectively. Individual tests on the same sample show relatively small variations in sound absorption coefficients of both foams. Therefore, the sound absorption coefficients of foams were represented as the average of two tests.

As depicted on Figures 7.11 (a) and (b), the sound absorption coefficients increase as the frequency increases. Figures 7.12 (a) and (b) show the sound absorption coefficient variations of Al and SiC/Al foams of varying relative densities as function of frequency, respectively. As the relative density increases, as it is expected, sound absorption coefficient values decrease and the increases in sound absorption values are more pronounced at higher frequencies. The highest sound absorption coefficient of Al foam sample is found 0.5 at the lowest relative density value of 0.0492. Within the studied relative density range: however, Al foams showed sound absorption coefficients well below 0.5. SiC/Al foam showed higher sound absorption coefficients, the highest sound absorption coefficient is found 0.74 at the lowest relative density value of 0.04. The sound drop level in Al and SiC/Al foam samples with the highest sound absorption

coefficient values were calculated as 3.0 dB and 5.85 dB, for Al and SiC/Al foams, respectively, using the following equation (Lu et al. 1999):

$$\Delta^* = 10 \log_{10}(1-\alpha) \tag{7.5}$$

where Δ^* is the sound drop level. It is also noted that although at low relative densities, less than 0.05, the sound absorption coefficients of Al and SiC/Al foams are comparable (Figure 7.13) at increasing relative densities and frequencies SiC/Al foam show higher sound absorption coefficients (Figures 7.14). The sound absorption measurements of undrilled Al and SiC/Al foam samples are listed in Appendix B.
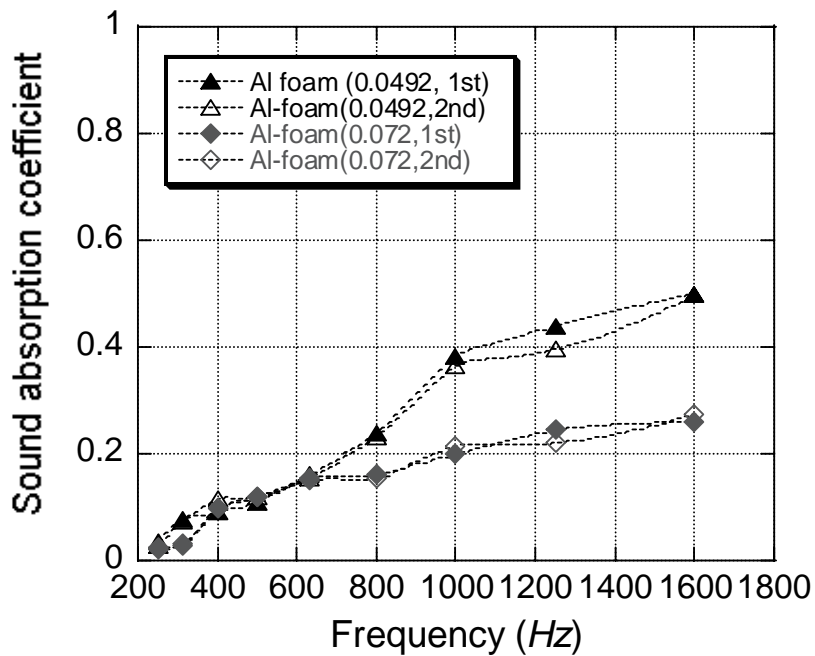
(a)
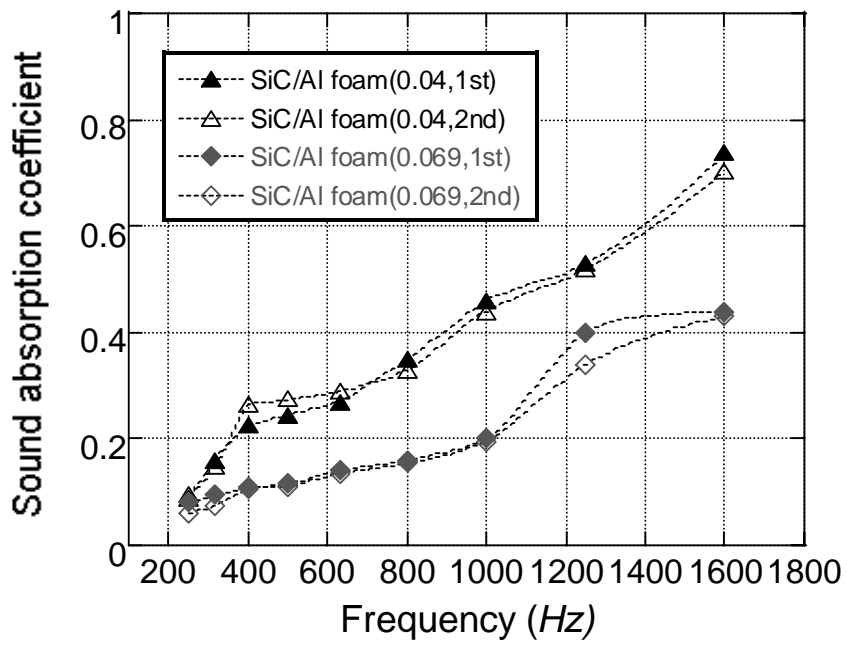
(b)

Figure 7.11. Comparison of sound absorption tests results of (a) Al foams and
(b) SiC/Al foams conducted on the same samples.

(a)

(b)
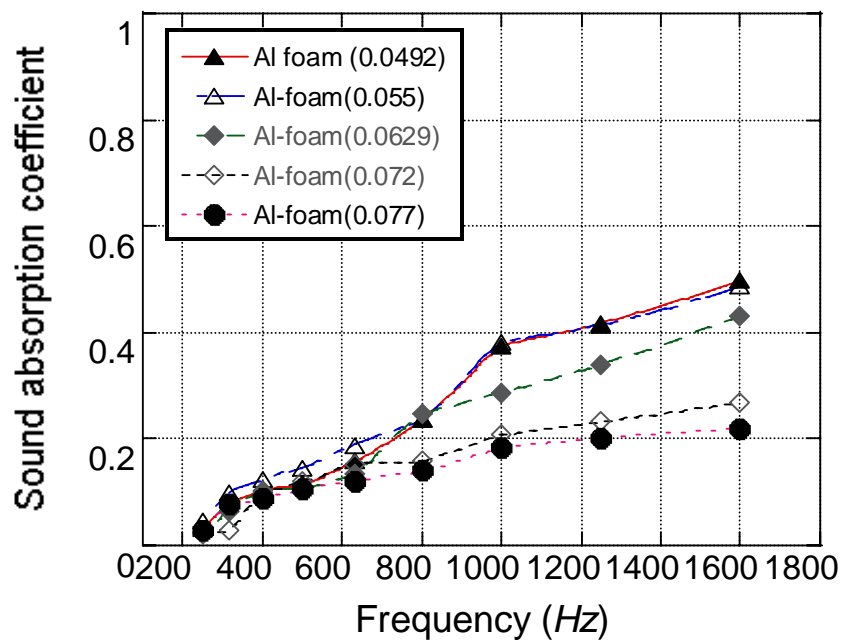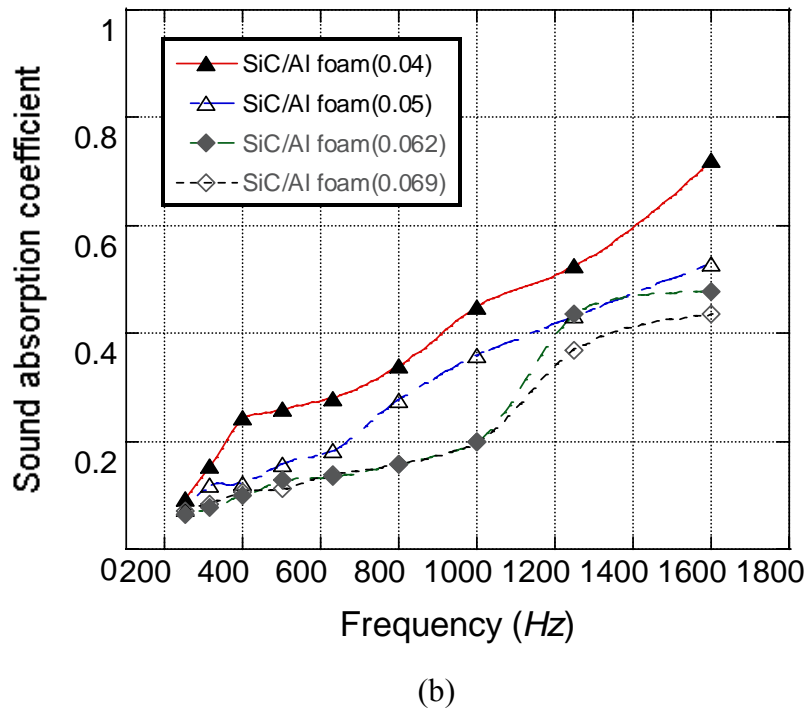
Figure 7.12. Sound absorption coefficients of Al and SiC/Al foams as function of frequency at different relative densities (a) Al foam and (b) SiC/Al foam.
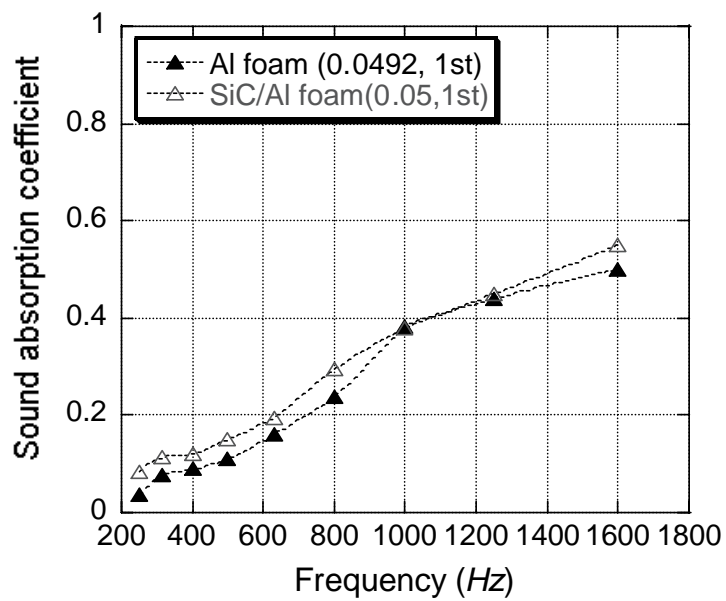
Figure 7.13. Comparison of sound absorption coefficients of Al and SiC/Al foam at relatively low relative densities.
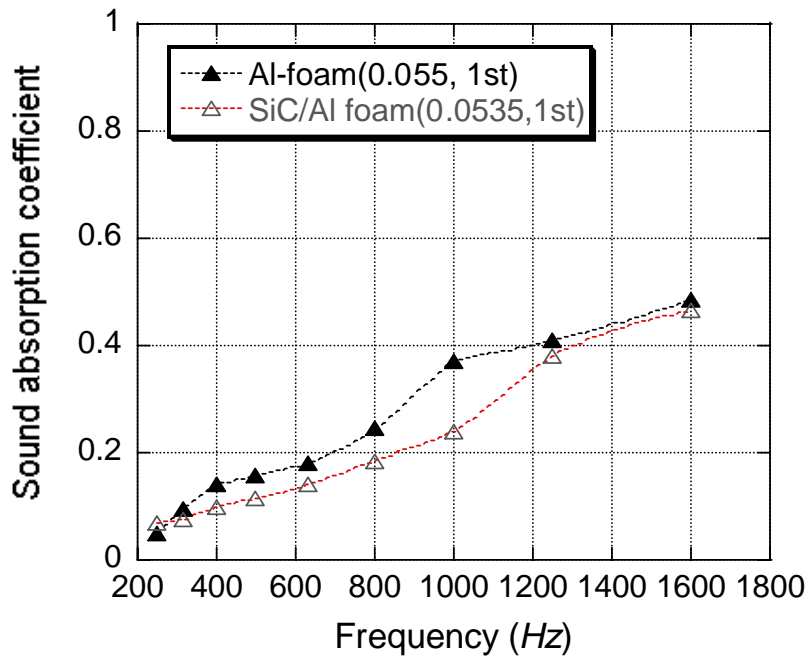
(a)
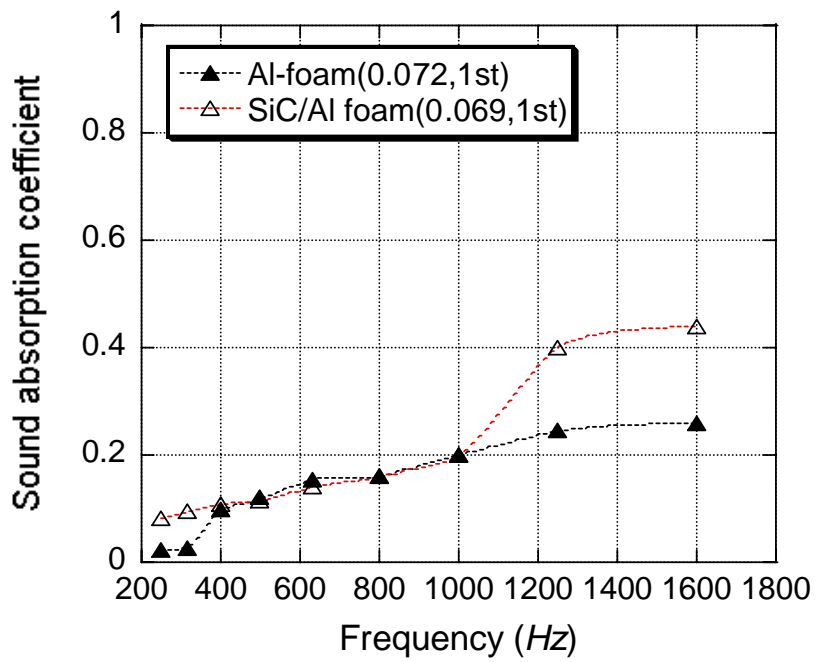
(b)

Figure 7.14. Comparison of sound absorption coefficients of Al and SiC/Al foam at about (a) 0.055 and (b) 0.07 relative densities.

Figure 7.15 shows a perfect sound absorber glass wool with a thickness of 50 mm and backed by a rigid wall. Compared with Al and SiC/Al foams, glass wool have apparent higher absorb peak at selected frequencies (Lu et al. 1999). Above 1000 Hz, the sound absorption coefficient was almost 1 for glass wool, which means all the sound was absorbed by the material (Equation 7.5), however sound absorption coefficient values of Al and SiC/Al foams were 0.383 and 0.46, respectively, at the same frequency ranges. It could be concluded that both foam types were not good sound absorbers without any prior treatments.
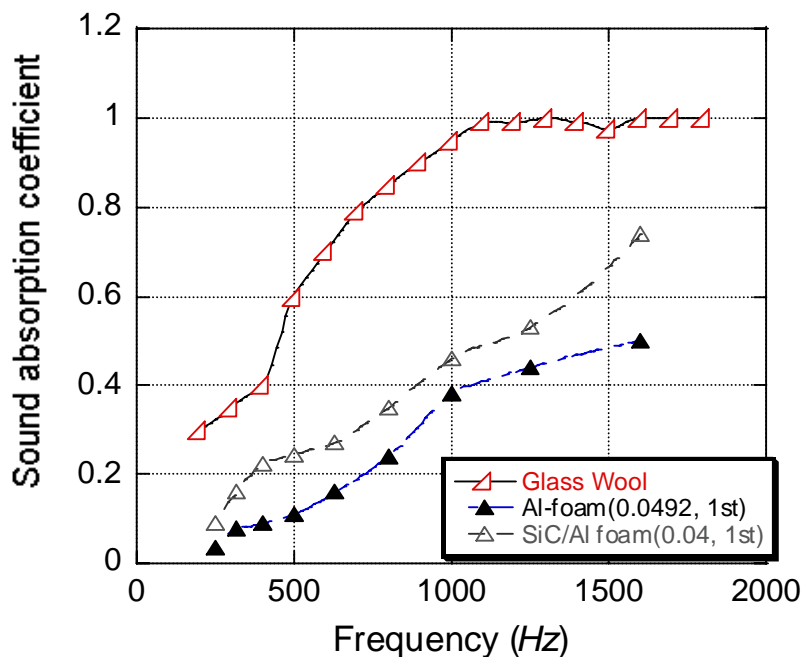
Figure 7.15. Comparison of sound absorption coefficients of 50-mm-thick glass–wool, 10-mm-thick Al and SiC/Al foams plotted as function of frequency.

7.5. Characteristic Sound Absorption Behavior of Al and SiC/Al Foams Subject to Hole Drilling

Figures 7.16 (a) and (b) shows the sound absorption coefficients of 10-mm-thick Al foam and SiC/Al foam samples with 1.5 and 2.5 mm hole drills, respectively. On the same figures the sound absorption coefficients of undrilled samples are also shown for comparison purposes. Hole drilling increases the sound absorption coefficients of foams

significantly and the sound is almost completely absorbed in the frequency range of 1000-1600 Hz as shown in Figures 7.16 (a) and (b). It is also noted that hole drilling becomes effective after 400 Hz and after this frequency the sound absorption coefficients increase rapidly over 0.8. These results suggest that hole drilling in relatively thin foam samples provide additional benefits for sound absorption. The sound absorption measurements of 1.5 and 2.5 mm hole drilled Al and SiC/Al foam samples are listed in Appendix B.

(a)

(b)
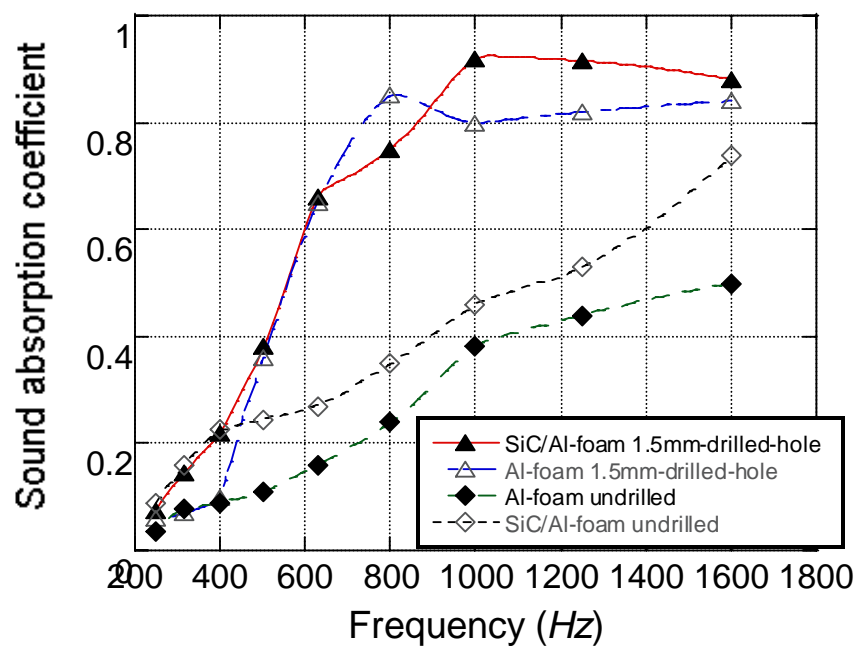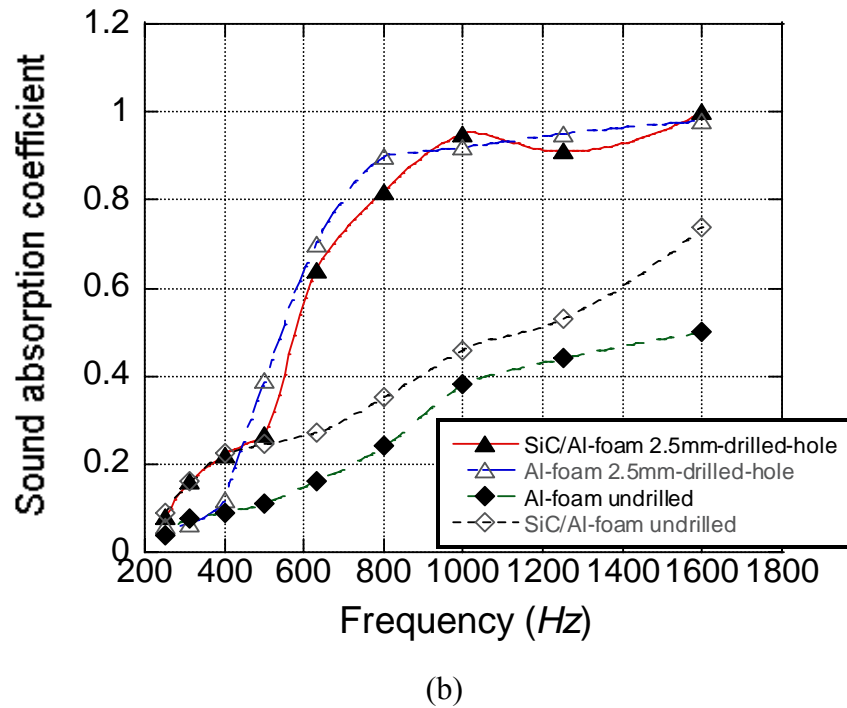
Figure 7.16. Comparison of sound absorption coefficients of undrilled and drilled
Al and SiC/AL foams (a) 1.5 mm-drilled-hole and (b) 2.5 mm-drilled-
hole Al and SiC/Al foams (the initial relative density of Al and SiC/Al
foams are 0.0492 and 0.04, respectively).

The experimental results presented above clearly show that the sound absorption coefficients of Al and SiC/Al can be increased significantly through hole drilling. It is well known that foams have higher damping capacity and natural vibration frequencies than the solid of which they are made. As discussed before in Chapter 5, the mechanisms of sound absorption include, (a) viscous losses as the pressure wave pumps air in and out of cavities in the absorber, (b) thermal-elastic damping, (c) Helmholtz-type resonators, (d) vortex shedding from sharp edges, (e) direct mechanical damping in the material itself, and so on. The effect of mechanism of (e) on sound absorption is usually small in metal foams (Lu et al. 1999). The contribution of mechanism (d) to sound absorption may also be neglected if there is no mean flow associated with the sound. Therefore, sound absorption in metallic foams is mainly due to the mechanisms of (a), (b) and (c). It was shown in a previous study that, the Helmholtz-type resonators operated at relatively high frequencies far exceeding the frequency range investigated in this study (Lu et al. 1999). However, viscous and thermal effects are effective in

increasing the sound absorption capacity of the present foams up to 1000 Hz. At high frequency levels however thermal effects are expected to be dominant. The slight increase in the sound absorption coefficient of SiC/Al foams may be attributed to the presence of SiC particles on the cell wall surfaces as shown in Figures 7.17 (a) and (b) leading to higher thermal elastic damping. The interaction of sound waves with the crushed cell walls of the drilled samples is shown schematically in Figure 7.18. The sound wave is partly reflected and absorbed by the crushed cells and due to the presence of SiC particles on the opened cell walls a slightly higher sound absorption coefficient values are found in SiC/Al foams due to the thermal elastic damping. It should be noted that viscous losses are only effective at thicker specimens, above 10 cm.

(a)   (b)
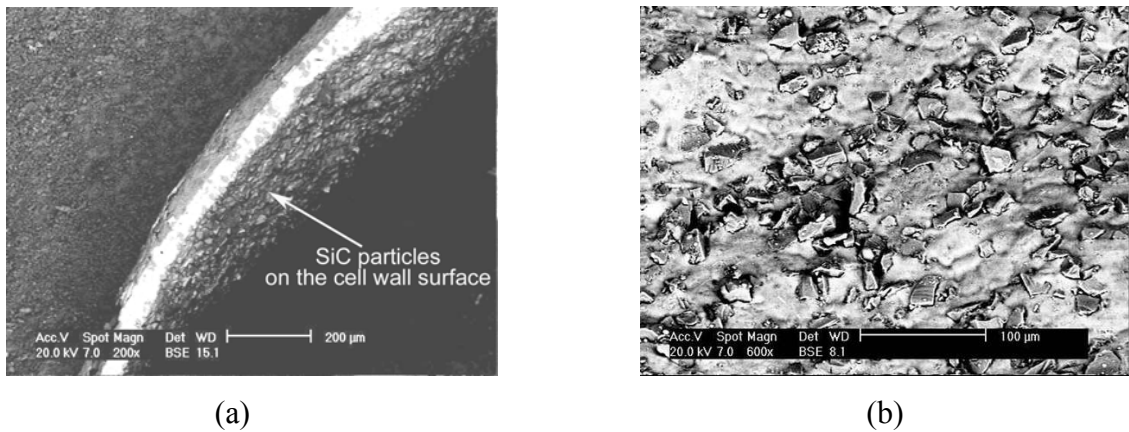
Figure 7.17. Scanning electron microscope images of SiC/Al foam sample cell wall surfaces (a) low and (b) high magnifications.
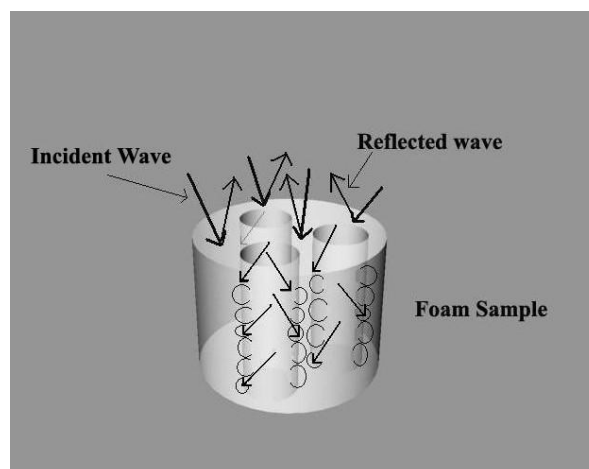
Figure 7.18. Schematic view of sound absorption in drilled foam samples.

CHAPTER 8

CONCLUSIONS

An experimental study has been conducted to investigate the effective thermal conductivity and sound absorption coefficient of Al and $SiC_{particle}$/Al closed-cell foams. The foams were prepared in house using the foaming of powder compact processes developed by Fraunhofer CMAM. The foaming of powder compact process has been extended for the foaming of composite compacts containing 10 weight percent of SiC particles. The porosity levels of foams varied between 86% and 96%. The measured ETCs of the foams were also fitted to the previously developed ETC models of metal foam. The ETC values of Al foams were also compared with those of Alporas closed and ERG open cell foams produced by the foaming of Al melt and investment casting methods, respectively. The effect of hole drilling on the sound absorption coefficients of foams were investigated by testing the foams samples contained 1.5 mm and 2.5 mm longitudinal drilled holes. Based on the experimental results of effective thermal conductivity and sound absorption coefficients measurements followings may be concluded;

1. The ETC values of SiC/Al foams were found lower than those of Al foams. The difference decreased as the porosity increased from 86% to 91% porosity level. At high porosity levels, above 91%, the ETC of SiC/Al foams reached the ETC of Al foams.

2. The lower ETC of composite foam was attributed to the lower thermal conductivity of the SiC particulates. At increasing porosity levels the lower thermal conductivity of the air was dominant on the ETC of the foams.

3. Following equations could be used to predict the ETCs of foams with sufficiently high regression constants:

$$k_e = k_{parallel}{}^{A} \cdot k_{series}{}^{(1-A)}$$

where, $A=11.449-23.692\,\phi+13.194\,\phi^2$ for Al foam and

$A=17.943-38.596\,\phi+21.722\,\phi^2$ for SiC/Al foam.

4. The present Al foams showed lower ETC values as compared with Alporas closed and ERG open cell foams. This was attributed to the oxide filaments, which were the remnants of thin oxide layer on surfaces of the original Al particles. Microscopic analysis of the cell walls showed that the oxide boundaries between the original particles were retained on the cell walls.

5. The sound absorption coefficients of Al and SiC/Al foams were found relatively low and similar at lower relative densities and frequencies.

6. The sound absorption coefficient of SiC/Al foams became slightly higher at increasing frequency levels above 1000 Hz.

7. Hole drilling was found to be effective in increasing sound absorption values of foam above 400 Hz. Following this critical frequency level, the sound absorption coefficients of foams increased rapidly over 0.8 in the drilled foam samples.

8. These results confirmed the previous studies in that the hole drilling provided additional benefits for the sound absorption in relatively thin foam samples.

9. The sound absorption in Al and SiC/Al foams was explained based on the viscous losses and thermal damping effects.

REFERENCES

Amjad, S., 2001. "Thermal Conductivity and Noise Attenuation in Aluminum Foams", Master Thesis, University of Cambridge, (October 2001), Cambridge, pp. 22-23.

Ashby, M.F., Evans, A., Fleck, N.A., Gibson, L.J., Hutchinson, J.W. and Wadley, H.N.G., 2000. "Metal Foams – A design guide". *Butterworth-Heinemann.* United States. pp. 181-186.

Babcsa´n, N., Me´sza´ros, I. and Hegman, N., 2003. "Thermal and electrical conductivity measurements on aluminum foams", *Mat.-wiss.u.Werkstofftech.* Vol. 34, pp. 391–394.

Banhart, J. and Baumeister, J. 1998. "Production Methods for Metallic Foams", MRS Symposium Proceeding, San Francisco, Vol. 521, pp. 121-132.

Banhart, J., 1999. "Applications in transportation, Functional applications", Hahn-Meitner-Institut Berlin-Germany, *International Journal of Vehicle Design*. pp. 1-13.

Banhart, J., 2000. "Manufacturing routes for metallic foams", *JOM*. Vol. 52, pp. 22- 27.

Banhart, J., 2000. "Metallic foams: challenges and opportunities", Eurofoam, *MIT-Verlag, Bremen*. pp. 13-20.

Banhart, J., 2003. "Aluminum foam for Lighter Vehicles", Hahn-Meitner-Institut Berlin-Germany, *International Journal of Vehicle Design*. pp. 1-19.

Baumeister, J., Schrader, H., 1992. *US Patent* No. 5151246.

Baumeister, J., 2000. *Sandwich Construction 5*, (EMAS, Solihull-United Kingdom), Vol. 1, p. 339.

Baumgärtner, F., Duarte, I. and Banhart, J., 2000. "Industrialization of powder compact foaming process", *Advanced Engineering Materials*. Vol. 2, pp. 168-174.

Beranek, L. L. and Ver, I. L., 1992. *Noise and Vibration Control Engineering*, (John Wiley & Sons Inc, New York), p.87.

Bhattacharya, A., Calmidi, V.V. and Mahajan, R.L., 1999. "An Analytical-Experimental Study for the determination of the effective thermal conductivity of high porosity fibrous foams", Application of Porous Media Methods for Engineered Materials*, ASME*. Vol. 233, pp. 13-20.

Bhattacharya, A., Calmidi, V. V. and Mahajan, R. L., 2002. "Thermophysical properties of high porosity metal foams", *International Journal of Heat and Mass Transfer*. Vol. 45, pp. 1017 –1031.

Biermann, J. W., 2004. "Opening and closing door noise and the performance of metal foam in automobiles", New technology Symposium, Aachen University-Germany, (15 October-16 October 2004), pp. 1-2.

Boomsma, K., Poulikakos, D., 2001. "On the effective thermal conductivity of a three-dimensionally structured fluid-saturated metal foam", *International Journal of Heat and Mass Transfer*. Vol. 44, pp. 827-836.

Boomsma, K., Poulikakos, D. and Zwick, F., 2003. "Metal Foams as Compact high Performance Heat Exchangers", *Mechanics of Materials*. Vol. 35, pp. 1161-1176.

Brown, S., 2000. "Sound Attenuation", in *On-Site Power Generation, A Reference Book*, Third Edition, (Electrical Generating Systems Association Press), pp. 67-101.

Calmidi, V. V. and Mahajan, R. L., 1999. "The Effective Thermal Conductivity of High Porosity Fibrous Metal Foams", *ASME Journal of Heat Transfer*. Vol. 122, (May 1999), pp. 466-471.

Daryabeigi, K., 1999. "Analysis and Testing of High Temperature Fibrous Insulation for Reusable Launch Vehicles", 37th AIAA Aerospace Sciences Meeting and Exhibit, AIAA, Virginia (11 January-14 January 1999), pp. 11-14.

Eisenmann, M., 1998. "Metal Powder Technologies and Applications", in *ASM Handbook*, (ASM International, Materials Park-USA), Vol. 7, pp. 1031-1042.

Elbir, S., 2001. "Preparation and characterization of aluminum composite closed cell foams", Master Thesis, Izmir Institute of Technology.

Fernández, L. and Wittig, H., 2003. "Foam Applications in the Automotive Sector", Trocellen Group Syposium, Madrid, (4 May- 6 May 2003), Physically Cross Linked Foams Automotive Technology International, pp. 1-2.

French, A. P., 1971. *Vibrations and Waves*, (Thomas and Sons ltd., MIT), pp. 264-267.

Fuganti, A., Lorenzi, L., Hanssen, A. G. and Langseth, M., 2000. "Aluminum foam for automobile applications", *Advanced Engineering Materials*. Vol. 2, pp. 200-204.

Gergely, V. and Clyne, B., 2000. "The Formgrip process: foaming of reinforced metals by gas release in precursors", *Advanced Engineering Materials*. Vol. 2, No: 4, pp. 175-178.

Gergely, V., Curran, D.C. and Clyne, T.W., 2003. The Foamcarp process, *Comp. Sci. and Technology*, in press.

Gibson, L. J. and Ashby, M. F., 1997. *Cellular Solids, Structures and Properties*, , (Cambridge University Press Ltd.), Second Edition, pp. 151-161.

Gibson, L. J. and Simone, A. E.,1997. "Aluminum Foams: Structure and Properties", Mechanics and Materials Seminar, (3 April 1997), pp 16-19.

Han, F., Seiffert, G., Zhao, Y. and Gibbs, B., 2003. "Acoustic absorption behavior of an open-celled aluminum foam", *Journal of Physics D: Applied Physics*. Vol. 36, pp. 294-302.

Hanssen, A.G., Langseth, M. and Hopperstad, O.S., 2000. "Static and dynamic crushing of square aluminum extrusions with aluminum foam filler", *Int. J. Impact Eng.*. Vol 24(200), pp. 347-383.

Hegman, N. and Babcsán, N., 2005. "Specific Feature of Thermal and Electrical Transport in Cellular Media". pp. 1-7.

Holman, J, 2002. *Heat Transfer*, (McGraw-Hill Companies Inc.), Ninth edition, pp. 5-9, 9-12, 12-13.

Huebelt, J., Zeibig, A., Kostmann, C. and Stephani, G., "Parameter of metallic hollow spheres - a porous sound absorbing material". pp. 1-4.

Hunt, M. L. and Tien, C. L., 1988. "Effects of Thermal Dispersion on Forced Convection in Fibrous Media", *International Journal of Heat and Mass Transfer*. Vol. 31, pp. 301-309.

Kakaç, S., 1998. *Isı Transferine Giriş-1, Isı İletimi*, (Tıp&Teknik Yayıncılık-Ankara), pp. 11-27.

Kavi, H., 2004. "Investigation of compression mechanical behavior of aluminum foam filled metal tubes", Master Thesis, Izmir Institute of Technology.

Körner C. and Singer F. R., 2000. "Processing of Metal Foams − Challenges and Opportunities, Advanced engineering materials", *Advanced Engineering Materials*. Vol. 2, No. 4, pp. 159-165.

Lam, Y. W., 1995. "Room Acoustics", *Acoustics of Enclosed Spaces*. pp. 1-11.

Leitlmeier, D., Degischer, H.P. and Flankl, H.J., 2002. "Development of a Foaming Process for Particulate Reinforced Aluminum melts", *Advanced Engineering Materials*. Vol. 4, pp. 735-740.

Lienhard IV, J. H. and Lienhard V, J. H., 2001. *A Heat Transfer Textbook*, (Phlogiston Press, Cambridge-Massachusetts), pp. 656-677.

Lord Rayleigh, 1892. *On the influence of obstacles arranged in rectangular order upon the properties of a medium*, Phil. Mag. L VI, pp. 481-502.

Lu, T. J., Hess A. and Ashby, M. F., 1999. "Sound absorption in metallic foams", *Journal of Applied Physics*, (1 June 1999). Vol. 85, No. 11, pp. 7528-7539.

Maxwell, J.C., 1873. *A Treatise on Electricity and Magnetism*, (Clarendon Press, Oxford), p. 365.

Miyoshi, T., Itoh, M., Akiyama, S. and Kitahara, A., 2000. "Alporas aluminum foam: production process, properties, and applications", *Advanced Engineering Materials*. Vol. 2, No: 4, pp. 179- 183.

Nakamura, T., Gnyloskurenko, S. V., Sakamoto, K., Byakova and Ishikawa, R., 2002. "Materials Transaction". Vol. 43, pp. 1191-1196.

Pain, H. J., 1993. *The Physics of Vibrations and Waves*, (John Wiley, New York), Fourth Edition, pp. 144-163.

Park, J., Palumbo, D.L., 2004. "Measurements of acoustic properties of porous and granular materials and application to vibration control". pp. 1-10.

Prakash, O., Sang, H. and Embury, J. D., 1995. "Structure and properties of Al-Si foam", *Material. Science Engineering*. Vol. 199, pp. 195-203.

Raju, S., 2003. "Noise Pollution and Automobiles", Symposium on International Automotive Technology, New York, (14 May-16 may 2003), pp. 57-61.

Singh, R, Kasana, H.S., 2004. "Computational aspects of effective thermal conductivity of highly porous metal foams", *Applied Thermal Engineering*. Vol. 24, pp. 1841-1849.

Sullines, D. and Daryabeige, K., 2001. "Effective Thermal Conductivity of High Porosity Open Cell Nickel Foam", Proceeding, 35th AIAA Thermophysics Conference, Anaheim, CA, pp 10-11.

Urban, P., 2004. "Body acoustics and noise reduction in automobiles", Volkswagen Group, Body acoustic workshop, Berlin, (8 May 2004), pp.11-14.

Vafai, K. and Tien, C. L., 1982. "Boundary and Inertia Effects on Convective Mass Transfer in Porous Media", *International Journal of Heat and Mass Transfer*. Vol. 25, pp. 1183-1190.

Wadley Haydn, N.G., 2002. "Cellular Metals Manufacturing", *Advanced Engineering Materials*. Vol. 4, No. 10, pp. 726-733.

WEB_1, 2005. Dave Curran Metal foams, 10/02/2005. http://www.msm.cam.ac.uk /mmc/people/dave/dave. html

WEB_2, 2003. Product information of Duocel and ERG Inc., Oakland (USA), 19/09/2003. http://www.ergaerospace.com

WEB_3, 2005. The UK's National Measurement Laboratory. 15/03/2005. http://www.npl.co.uk/materials/metal_foams/applications.html

WEB_4, 2005. Leaders in Soundproofing, Noise and Vibration, 24/01/2005. http://soundproof. mine.nu/

WEB_5, 2004. Product data sheet of Recemat, SEAC International B.V., (Netherlands), 27/08/2004. http://www.seac.nl

Woodack, R, 2000. *Brüel & Kjær Standing Wave Apparatus Type 4002 User Manual*, (CapGerard Press., London), Sixth Edition, pp. 28-32.

Writz, R. A., 1997. "A Semi-Empirical Model for Porous Media Heat Exchanger Design", Proceedings of the American Society of Mechanical Engineers National Heat Transfer Conference, Baltimore, MD, pp. 44-58.

Xu, M. B., Selamet, A. and Lee, I.-J., 2004. "Analytical approach for sound attenuation in perforated dissipative silencers", *Journal of Acoustical Society of America.* pp. 2091–2099.

Yu, C., Eifert, H., Banhart, J. and Baumeister, J., 1998. "Metal foaming by a metallurgy method: production, properties and applications", *Journal of Materials Research Innovations*. Vol. 2, p. 3.

Yuksel, S. and Guden, M., 2005. "SiC-particulate aluminum composite foams produced by powder compacts: foaming and compression behavior", *Journal of Materials Science*, in press.

Zhao, C. Y., Lu, T. J., Hodson, H. P. and Jackson, J. D., 2004. "The Temperature Dependence of Effective Thermal Conductivity of Open-Celled Steel Alloy Foams". Vol. 367, pp. 123-131.

Ziomek, J. L., 1995. *Fundamentals of Acoustic Field Theory and Space-Time Processing*, (CRC Pressing, New York), pp. 3-4, 40-41.

APPENDIX A

Al AND COMPOSITE FOAM SAMPLES PREPARED FOR ETC MEASUREMENTS AND EXPERIMENTAL ETC RESULTS

Table A.1. Al foam samples prepared for ETC measurements.

Al-foam Samples	Density (g/cm^3)	d_{rel}	Porosity (%)	Cell size (mm)	Mass (g)
No.1	0.360	0.133	86.7	2-2.5	5.30
No.2	0.330	0.122	87.8	2-2.5	4.86
No.3	0.327	0.121	87.9	2-2.5	4.815
No.4	0.290	0.107	89.3	1.5-2	4.27
No.5	0.361	0.134	86.6	2-2.5	5.31
No.6	0.298	0.110	89.0	2-2.5	4.38
No.7	0.235	0.087	91.3	1.5-2	3.46
No.8	0.310	0.115	88.5	2-2.5	4.565
No.9	0.290	0.107	89.3	1.5-2	4.27
No.10	0.271	0.100	90.0	1.5-2	3.99
No.11	0.322	0.119	88.1	2-2.5	4.74
No.12	0.307	0.113	88.7	2-2.5	4.521
No.13	0.313	0.116	88.4	2-2.5	4.60
No.14	0.317	0.117	88.3	2-2.5	4.66
No.15	0.318	0.118	88.2	2-2.5	4.683
No.16	0.247	0.0915	90.85	1.5-2	3.63
No.17	0.227	0.084	91.6	1.5-2	3.343
No.18	0.209	0.0774	92.26	1.5-2	3.07
No.19	0.384	0.142	85.8	2-2.5	5.655
No.20	0.269	0.0996	90.04	1.5-2	3.96
No.21	0.376	0.139	86.1	2-2.5	5.53
No.22	0.382	0.1415	85.85	2-2.5	5.62
No.23	0.370	0.137	86.3	2-2.5	5.449
No.24	0.325	0.120	88.0	2-2.5	4.78
No.25	0.370	0.137	86.3	2-2.5	5.449
No.26	0.371	0.1374	86.26	2-2.5	5.46
No.27	0.329	0.1219	87.81	2-2.5	4.83
No.28	0.357	0.132	86.8	2-2.5	5.25
No.29	0.245	0.090	91.0	1.5-2	3.608

Table A.2. SiC/Al foam samples prepared for ETC measurements.

SiC/Al-foam Samples	Density (g/cm^3)	d$_{rel}$	Porosity (%)	Cell size (mm)	Mass (g)
No.30	0.210	0.0764	92.4	1.5-2	3.09
No.31	0.220	0.08	92.0	1.5-2	3.24
No.32	0.247	0.089	91.1	1.5-2	3.63
No.33	0.271	0.0985	90.15	1.5-2	3.99
No.34	0.290	0.1054	89.46	1.5-2	4.27
No.35	0.310	0.1127	88.7	2-2.5	4.565
No.36	0.320	0.1163	88.4	2-2.5	4.71
No.37	0.360	0.131	86.9	2-2.5	5.30
No.38	0.280	0.102	89.8	1.5-2	4.12
No.39	0.370	0.1345	86.55	2-2.5	5.449
No.40	0.380	0.1381	86.2	2-2.5	5.59
No.41	0.330	0.12	88.0	2-2.5	4.86
No.42	0.370	0.1345	86.55	2-2.5	5.449
No.43	0.270	0.0981	90.2	1.5-2	3.97
No.44	0.255	0.093	90.7	1.5-2	3.75
No.45	0.255	0.093	90.7	1.5-2	3.75
No.46	0.290	0.1054	89.5	1.5-2	4.27
No.47	0.382	0.1389	86.1	2-2.5	5.62
No.48	0.384	0.1396	86.04	2-2.5	5.65
No.49	0.380	0.1381	86.2	2-2.5	5.59
No.50	0.360	0.131	86.9	2-2.5	5.30
No.51	0.360	0.131	86.9	2-2.5	5.30
No.52	0.291	0.1058	89.4	1.5-2	4.285
No.53	0.370	0.1345	86.55	2-2.5	5.449
No.54	0.315	0.1145	88.55	2-2.5	4.639
No.55	0.300	0.109	89.1	2-2.5	4.418
No.56	0.241	0.0876	91.2	1.5-2	3.55
No.57	0.316	0.1149	88.5	2-2.5	4.65
No.58	0.325	0.1181	88.2	2-2.5	4.78
No.59	0.245	0.0891	91.09	1.5-2	3.61

Table A.3. Al foam samples effective thermal conductivity values (ETC).

Al-foam Samples	d_{rel}	Porosity (%)	Thermal conductivity k, (W/m·K) -expt.-
No.1	0.133	86.7	8.65
No.2	0.122	87.8	7.90
No.3	0.121	87.9	7.83
No.4	0.107	89.3	6.54
No.5	0.134	86.6	8.70
No.6	0.110	89.0	6.58
No.7	0.087	91.3	5.43
No.8	0.115	88.5	6.70
No.9	0.107	89.3	6.54
No.10	0.100	90.0	6.33
No.11	0.119	88.1	6.84
No.12	0.113	88.7	6.66
No.13	0.116	88.4	6.72
No.14	0.117	88.3	6.72
No.15	0.118	88.2	6.75
No.16	0.0915	90.85	5.78
No.17	0.084	91.6	5.40
No.18	0.0774	92.26	5.13
No.19	0.142	85.8	9.18
No.20	0.0996	90.04	5.94
No.21	0.139	86.1	8.87
No.22	0.1415	85.85	9.15
No.23	0.137	86.3	8.78
No.24	0.120	88.0	6.80
No.25	0.137	86.3	8.78
No.26	0.1374	86.26	8.80
No.27	0.1219	87.81	7.86
No.28	0.132	86.8	8.62
No.29	0.090	91.0	5.61

Table A.4. SiC/Al foam samples effective thermal conductivity values (ETC).

SiC/Al-foam Samples	d_{rel}	Porosity (%)	Thermal conductivity k, (W/m·K) -expt.-
No.30	0.0764	92.4	5.01
No.31	0.08	92.0	5.04
No.32	0.089	91.1	5.06
No.33	0.0985	90.15	5.23
No.34	0.1054	89.46	5.48
No.35	0.1127	88.7	5.71
No.36	0.1163	88.4	5.89
No.37	0.131	86.9	6.94
No.38	0.102	89.8	5.32
No.39	0.1345	86.55	7.18
No.40	0.1381	86.2	7.44
No.41	0.12	88.0	6.65
No.42	0.1345	86.55	7.18
No.43	0.0981	90.2	5.18
No.44	0.093	90.7	5.1
No.45	0.093	90.7	5.1
No.46	0.1054	89.5	5.48
No.47	0.1389	86.1	7.5
No.48	0.1396	86.04	7.64
No.49	0.1381	86.2	7.44
No.50	0.131	86.9	6.94
No.51	0.131	86.9	6.94
No.52	0.1058	89.4	5.52
No.53	0.1345	86.55	7.18
No.54	0.1145	88.55	5.80
No.55	0.109	89.1	5.41
No.56	0.0876	91.2	5.05
No.57	0.1149	88.5	5.82
No.58	0.1181	88.2	5.98
No.59	0.0891	91.09	5.07

APPENDIX B

Al AND COMPOSITE FOAM SAMPLES PREPARED FOR SOUND ABSORPTION MEASUREMENTS AND SOUND ABSORPTION MEASUREMENT RESULTS

Table B.1. Al foam samples prepared for sound absorption measurements.

Al-foam Samples	Density g/cm^3	d_{rel}	Porosity (%)	Cell size (mm)	Diameter (mm)	Thickness (mm)
No 61	0.133	0.0492	95.07	1.5-2	30	10
No 60	0.150	0.055	94.4	1.5-2	29.98	10
No 62,68	0.155	0.0574	94.25	1.5-2	30	10
No 63,69	0.167	0.06185	93.81	1.5-2	29.97	10
No 64	0.170	0.0629	93.7	1.5-2	30	10
No 65,66	0.195	0.072	92.7	1.5-2	30	10
No 69,70	0.208	0.077	92.29	1.5-2	30	10

Table B.2. SiC/Al foam samples prepared for sound absorption measurements.

SiC/Al-foam Samples	Density g/cm^3	d_{rel}	Porosity (%)	Cell size (mm)	Diameter (mm)	Thickness (mm)
No 71,72	0.110	0.04	96	1.5-2	30	10
No 73,76,77	0.120	0.0436	95.64	1.5-2	30	10
No 74	0.135	0.05	95	1.5-2	29.98	10
No 75,78	0.145	0.0527	94.7	1.5-2	30	10
No 80	0.147	0.0535	94.65	1.5-2	30	10
No 79	0.160	0.058	94.2	1.5-2	29.98	10
No 81,84,86	0.170	0.062	93.8	1.5-2	29.92	10
No 82,83,85	0.190	0.069	93.1	1.5-2	30	10

Table B.3. Sound absorption measurements of Al foam samples (including 2nd test).

Al-foam Samples	Density g/cm^3	d_{rel}	Porosity (%)	Cell size (mm)	Diameter x Thickness (mm)	Sound absorption coefficient, α	Sound absorption coefficient, α (2nd test)	Frequency (Hz)
No 60	0.150	0.055	94.5	1.5-2	29.98 x 10	0.048	0.044	250
						0.095	0.1	315
						0.14	0.11	400
						0.158	0.135	500
						0.18	0.198	630
						0.245	0.228	800
						0.37	0.39	1000
						0.41	0.42	1250
						0.485	0.488	1600
No 61	0.133	0.0492	95.07	1.0	30 x 10	0.037	0.028	250
						0.078	0.075	315
						0.090	0.115	400
						0.11	0.12	500
						0.16	0.155	630
						0.24	0.233	800
						0.383	0.365	1000
						0.44	0.3958	1250
						0.5	**0.498**	1600
No 62-68	0.155	0.0574	94.25	1.5-2	30 x 10	0.031	0.033	250
						0.084	0.077	315
						0.11	0.098	400
						0.125	0.105	500
						0.20	0.195	630
						0.215	0.21	800
						0.375	0.345	1000
						0.44	0.405	1250
						0.35	0.395	1600
No 63-69	0.167	0.0618	93.81	1.5-2	29.97 x 10	0.0295	0.0325	250
						0.069	0.065	315
						0.088	0.08	400
						0.105	0.1	500
						0.160	0.14	630
						0.21	0.19	800
						0.36	0.29	1000
						0.375	0.36	1250
						0.48	0.48	1600
No 64	0.170	0.0629	93.7	1.5-2	30 x 10	0.03	0.02	250
						0.065	0.065	315
						0.11	0.095	400
						0.115	0.1	500
						0.15	0.12	630
						0.245	0.25	800
						0.295	0.28	1000
						0.35	0.33	1250
						0.445	0.42	1600

Table B.3. (cont.).

Al-foam Samples	Density g/cm³	d_{rel}	Porosity (%)	Cell size (mm)	Diameter x Thickness (mm)	Sound absorption coefficient, α	Sound absorption coefficient, α, (2nd test)	Frequency (Hz)
No 65-66	0.195	0.072	92.7	1.5-2	30 x 10	0.023 0.028 0.098 0.120 0.155 0.16 0.20 0.245 0.26	0.02 0.03 0.1 0.12 0.15 0.155 0.215 0.22 0.275	250 315 400 500 630 800 1000 1250 1600
No 67-70	0.208	0.077	92.29	1.5-2	30 x 10	0.025 0.085 0.095 0.11 0.123 0.135 0.2 0.215 0.225	0.03125 0.069 0.082 0.1 0.12 0.145 0.165 0.19 0.215	250 315 400 500 630 800 1000 1250 1600

Table B.4. Sound absorption measurements of SiC/Al foam samples
(including 2nd test).

SiC/Al-foam Samples	Density g/cm³	d_{rel}	Porosity (%)	Cell size (mm)	Diameter x Thickness (mm)	Sound absorption coefficient, α	Sound absorption coefficient, α, (2nd test)	Frequency (Hz)
No 71-72	0.110	0.04	96	0.5-1.0	30 x 10	0.09	0.095	250
						0.16	0.148	315
						0.225	0.265	400
						0.245	0.274	500
						0.27	0.29	630
						0.35	0.33	800
						0.46	0.44	1000
						0.53	0.52	1250
						0.74	**0.705**	1600
No 73–76–77	0.120	0.0436	95.64	1.5-2	30 x 10	0.085	0.075	250
						0.125	0.12	315
						0.195	0.165	400
						0.22	0.205	500
						0.26	0.233	630
						0.32	0.295	800
						0.41	0.37	1000
						0.47	0.46	1250
						0.59	0.56	1600
No 74	0.135	0.05	95	1.5-2	29.9 x 10	0.085	0.06	250
						0.115	0.12	315
						0.12	0.125	400
						0.15	0.165	500
						0.195	0.17	630
						0.295	0.26	800
						0.38	0.34	1000
						0.45	0.415	1250
						0.55	0.51	1600
No 75-78	0.145	0.0527	94.7	1.5-2	30 x 10	0.07	0.066	250
						0.115	0.076	315
						0.135	0.13	400
						0.14	0.15	500
						0.17	0.17	630
						0.25	0.19	800
						0.28	0.24	1000
						0.42	0.385	1250
						0.49	0.46	1600
No 80	0.147	0.0535	94.65	1.5-2	30 x 10	0.07	0.060	250
						0.076	0.078	315
						0.1	0.09	400
						0.115	0.11	500
						0.14	0.143	630
						0.185	0.188	800
						0.24	0.22	1000
						0.38	0.37	1250
						0.465	0.46	1600

(cont. on next page)

SiC/Al-foam Samples	Density g/cm^3	d_{rel}	Porosity (%)	Cell size (mm)	Diameter x Thickness (mm)	Sound absorption coefficient, α	Sound absorption coefficient, α, (2nd test)	Frequency (Hz)
No 81-84-86	0.170	0.062	93.8	1.5-2	29.92 x 10	0.065	0.0622	250
						0.085	0.07	315
						0.098	0.1	400
						0.135	0.12	500
						0.145	0.125	630
						0.16	0.155	800
						0.205	0.19	1000
						0.44	0.43	1250
						0.49	0.4687	1600
No 82-83-85	0.190	0.069	93.1	1.5-2	30 x 10	0.081	0.06115	250
						0.094	0.075	315
						0.108	0.1026	400
						0.115	0.11	500
						0.14	0.135	630
						0.16	0.154	800
						0.20	0.195	1000
						0.40	0.34	1250
						0.44	0.43	1600
No 79	0.160	0.058	94.2	1.5-2	29.98 x 10	0.08	0.06225	250
						0.095	0.075	315
						0.093	0.086	400
						0.125	0.12	500
						0.14	0.135	630
						0.205	0.19	800
						0.225	0.245	1000
						0.395	0.36	1250
						0.49	0.46	1600

Table B.5. Sound absorption measurements of Al foam samples (including 2nd test) subject to hole drilling.

Al-foam Sample	d_{rel}	Porosity (%)	Sound absorption coefficient, α	Sound absorption coefficient, α (2nd test)	Hole-drilled		Frequency (Hz)
					1.5 mm	2.5 mm	
No 61	0.0492	95.07	0.037	0.028	0.06	0.06	250
			0.078	0.075	0.07	0.065	315
			0.090	0.115	0.10	0.12	400
			0.11	0.12	0.36	0.19	500
			0.16	0.155	0.65	0.35	630
			0.24	0.233	0.85	0.50	800
			0.383	0.365	0.80	0.80	1000
			0.44	0.3958	0.82	0.88	1250
			0.5	**0.498**	**0.84**	**0.96**	1600

Table B.6. Sound absorption measurements of SiC/Al foam samples (including 2nd test) subject to hole drilling.

SiC/Al-foam Samples	d_{rel}	Porosity (%)	Sound absorption coefficient, α	Sound absorption coefficient, α (2nd test)	Hole-drilled		Frequency (Hz)
					1.5 mm	2.5 mm	
			0.09	0.095	0.075	0.08	250
			0.16	0.148	0.145	0.16	315
			0.225	0.265	0.22	0.22	400
No 71-72	0.04	96	0.245	0.274	0.38	0.266	500
			0.27	0.29	0.66	0.34	630
			0.35	0.33	0.95	0.52	800
			0.46	0.44	0.92	0.85	1000
			0.53	0.52	0.915	0.91	1250
			0.74	**0.705**	**0.88**	**1.00**	1600